THEORY OF WIDE-ANGLE PHOTOMETRY FROM STANDARD STARS.*

Peter D. Usher

Department of Astronomy

The Pennsylvania State University

University Park, PA 16802.

* Report III to the Large-Scale Phenomena Network
of the International Halley-Watch.

This work was supported by NASA Grant NAG 5-361
through the NASA-Goddard Space Flight Center, Greenbelt, Md.

October 1989

CONTENTS

TABLES

FIGURES

I. INTRODUCTION.

Wide-angle celestial structures, such as bright comet tails and nearby galaxies and clusters of galaxies, rely on photographic methods for quantified morphology and photometry, primarily because electronic devices with comparable resolution and sky coverage are beyond current technological capability. CCDs with pixel numbers measured in the millions have become commonplace, but fail by orders of magnitude in providing sky coverage for large structures with good resolution. Even computers are daunted by the task of processing bits of information numbered in the thousands of millions. The photographic process succeeds for all its obdurate properties, and a picture speaks a thousand megawords.

Nevertheless, seeing is not quite believing, because photographic density is not simply related to luminous intensity. Morphology is clearly dependent on photometry, particularly in non-linear parts of the response, and astrophysically important numbers are dependent on both. While stars of known magnitude can be used to calibrate images of other stars, their use in determining the surface brightnesses of extended images is not straightforward.

Brandt (1985) has emphasized that stars of known magnitude are natural calibrators that should lead to accurate calibration of photographic plates if a suitable theory is forthcoming, because in principle all the necessary information resides in the exposed emulsion. Rather than being an unavoidable hindrance to isophotometry, star images would play a pivotal role in calibration. While spot sensitometry is the canonical means of plate calibration, it is not always available on plates of interest, and suffers from its own intrinsic calibration problems.

The present work is an examination, more-or-less from first principles, of the problem of the photometry of extended structures and of how this problem may be overcome through calibration by photometric standard stars. Previous work is summarized in ¶II. In ¶III the perfect properties of the ideal field-of-view are

stated in the guise of a radiometric paraxial approximation, in the fond hope that fields-of-view of actual telescopes will conform. Fundamental radiometric concepts are worked through in ¶IV before the issue of atmospheric attenuation is addressed in ¶V. The independence of observed atmospheric extinction and surface brightness leads off the quest for formal solutions to the problem of surface photometry in ¶VI.

Methods and problems of solution are discussed in ¶VII. The development relies on the powerful method developed by Zou, Chen, and Peterson (1981), but puts it on a radiometrically sound footing by solving the problem of the radiometric zero-point, and by ensuring through conservation of energy that atmospheric extinction and the radiometrically related sky brightness are actually part of the solution. Standard star image profiles need not conform to any theoretical ideal, but images must not be too distorted (see §7.6); on all counts, the present formalism is comparatively assumption-free. In its final form, all quantities that appear are dimensionless as they should be.

Liller (1985) has raised the spectre of reciprocity failure (RF), and ¶VII does not shrink from it. Rather, the spectre is confronted in the spirit of standard stars and shown to be chimerical in that light, provided certain rituals are adopted. RF (and a good deal else besides) can be exorcised in future studies of comets provided that standard stars are inserted just as sensitometry spots are inserted.

After a brief discussion in ¶VIII of Baker-Sampson polynomials and the vexing issue of saturation, ¶IX embarks on a pursuit of actual numbers to be expected in real cases. While the numbers crunched are gathered ex nihilo, they demonstrate the feasibilty of Newton's method in the solution of this overdetermined, nonlinear, least square, multiparametric, photometric problem. This is no small feat, and should encourage future research.

¶X concludes the Report with a summary of Reports I and II (Dorband et al. 1985; Dorband and Usher 1985); the definition of the search area for photometric standards in the P/Halley path, and their incidence and usefulness in future photometric reduction, is described.

Errors of one sort or another are bound to exist in spite of my best intentions, and I apologize for them in advance; I would appreciate your communicating them to me.

II. OTHER METHODS.

The first step in the process of converting density to surface brightness is the digitization of the image (see e.g. Klinglesmith 1983). Spot size should be larger than the scattering radius and grain separation, but large enough to reduce the noise of the output. Stock and Williams (1962) review 3 methods of data acquisition: (i) schraffierkassette, (ii) Fabry photometry, and (iii) extrafocal images, and they discuss the advantages and shortcomings of each. In (i), a moving image introduces the Intermittency Effect (combined with RF too if images are both point and extended). In (ii), the image size of point and extended images is the same, but complex lens systems are needed. In (iii), extrafocal images destroy morphological information, but Stock and Williams make an interesting point: extrafocal images are useful calibration tools when imposed in a separate exposure of the same length on a portion of the plate different from an extended object of interest. This concept of separate standard star sequences is a precursor to our solution to the problem of RF for trailed standards on comet plates (§7.6), except that, in light of recent advances (e.g. ZCP, Klinglesmith and Rupp 1984; Warnock and Klinglesmith 1984, and this Report), there is no need for the images to be out of focus! Moreover, there is the added bonus that atmospheric extinction can be found as part of the solution (§6.3 et seq.).

Stock and Williams (1962) also discuss sensitometric spot and wedge calibration. This is far and away the most common method nowadays, but it has drawbacks (see Agnelli et al. 1979); the object and the calibrators are not simultaneously exposed, and ambient conditions are oftentimes different; also, the characteristic curve may differ from one part of the plate to another. In our proposed method, ambient conditions will be different only if outside conditions are different, and these are amenable to experimental control and are capable of being monitored. As for not having the H&D (or characteristic curve) the same from one part of the plate

to another, multiple exposures are necessary and desirable in any case. In fact, standard stars can be used to calibrate the wedges.

The methods of Kormendy (1973), Agnelli et al. (1979), and Feitzinger et al. (1983) depend on assumptions regarding the profiles of field stars. Image symmetry is desirable and assumed to be independent of apparent magnitude. Kormendy (1973) determines the magnitude zero-point by simultaneous photoelectric photometry of the sky. The methods are limited by their assumptions and complexity, and exiguous in their lack of simultaneous solutions for sky brightness and extinction. Owing to the crucial role played by the sky brightness in Type II detections and thus in the definition of morphological structure (e.g. Sandage 1972), it is essential that the faint end of the H&D curve be well defined, but Feitzinger et al. (1983) show that this is not easily accomplished.

Zou, Chen, & Peterson (1981) [herein ZCP] give a method for star profiles of arbitrary shape, and so allow somewhat for a less-than-perfect world. In the exemplification of their method, the zero-point of the calibration (which is de facto the background sky brightness) is assumed, and there is no allowance for atmospheric extinction. The methods of ZCP and Agnelli et al. (1979) have been implemented by Klinglesmith & Rupp (1984) and Warnock & Klinglesmith (1984), though the problem of the photometric zero-point, extinction, and sky brightness, remain. The great promise shown by the moment-sum method of ZCP has suggested to the Steering Committee of the IH-W LSPN that its applicability to P/Halley, and future comet apparitions, be examined.

III. THE RADIOMETRIC PARAXIAL APPROXIMATION.

Wide-field imagery is accomplished normally with telescopes of the classic Schmidt design. Such cameras are stopped at the center of curvature of a concave spherical mirror, and so produce images that are free of coma and astigmatism. But they are afflicted with spherical aberration, and this is reduced to fifth order by an aspheric corrector situated at the camera stop. Thus each image lies on an optical axis that passes through the camera stop, and on a spherical focal surface whose center is at the center of curvature of the primary mirror. The basic principle of the Schmidt system therefore is that the telescope has no preferred optical axis, and so yields excellent images to high order in all field directions (Bowen 1960).

Distance-to-center effects will arise however because the corrector has a preferred axis. Images far from the axis of optical symmetry will suffer losses in irradiance owing to vignetting. There is also a deterioriation of image quality owing to residual aberrations; for oblique incidence, the residual fifth-order spherical aberration sets the limit on the field-of-view for good images, and coma and astigmatism also develop owing to the relative tilt of the corrector.

In general, the Radiometric Paraxial Approximation (the RPA) is valid for those directions sufficiently close to the axis of optical symmetry that losses in irradiance are negligible. For example, the unvignetting field of the 48-inch Palomar Schmidt camera is about 5.4 degrees; even at the corners of the 14-inch square photographic plates, the loss of irradiance is estimated to be less than 0.2 mag. (Minkowski and Abell 1963).

In the RPA, aberrations affect surface photometry only through a loss of morphological discrimination, since radiometric theory accounts for all the energy. The photometry of point sources is similarly unaffected. A radiometric calibration of the entire FOV of the telescope can be accomplished by standard stars sufficient-

ly close to the direction of interest. An accurate morphological-photometric description of structures larger than the field either of negligible aberrations or negligible vignetting may in theory be achieved with the help of the spatial response of the camera to point sources, but this is beyond the scope of the present treatment. In addition, chromatic aberration is a fundamental limitation to the morphological discrimination of any camera with a refracting element, and is present even in the RPA.

IV. RADIOMETRY

§4.1 PIXEL RADIANCE

Let $L(\lambda)$ be the Spectral Radiance of a source at infinity incident upon a telescope of nominal aperture diameter D, focal length f, and effective collecting area $A_e = \frac{1}{4}\pi GD^2$. The function G accounts for geometrical effects such as vignetting and shadowing of the primary.

A pixel area $\sigma = f^2\Omega$ in the focal plane subtends a solid angle Ω of the sky. The radiance $L(\lambda)$ suffers losses owing to the transmittances $T_t(\lambda)$ and $T_f(\lambda)$ of the telescope and filter respectively. If the detector has a quantum efficiency $R_d(\lambda)$, then the System Response is:

$$S(\lambda) = T_t(\lambda)\cdot T_f(\lambda)\cdot R_d(\lambda). \tag{4.1.1}$$

The detected spectral radiance is:

$$F(\lambda) = L(\lambda)\, S(\lambda), \tag{4.1.2}$$

and the detected Spectral Illumination is:

$$I(\lambda) = \int_{\Omega} F(\lambda)\, d\omega. \tag{4.1.3}$$

The heterochromatic Illumination is found by integration over the bandpass of the system response; this bandpass is symbolically represented by β. Thus:

$$I(\beta) = \int_{\beta} I(\lambda)\, d\lambda = \int_{\beta}\int_{\Omega} F(\lambda)\, d\lambda\, d\omega\ . \tag{4.1.4}$$

The heterochromatic Power detected is:

$$P(\beta) = A_e\, I(\beta) = A_e \int_{\beta}\int_{\Omega} F(\lambda)\, d\lambda\, d\omega, \tag{4.1.5}$$

assuming A_e to be independent of λ and ω. The total Energy detected over integration time T is:

$$Q(\beta) = A_e \int_{T} I(\beta)\, dt = A_e \int_{T}\int_{\beta}\int_{\Omega} F(\lambda)\, dt\, d\lambda\, d\omega\ . \tag{4.1.6}$$

Each integration in Equation (4.1.6) entails loss of information; in self-explanatory notation, appropriate mean quantities are:

$$(4.1.7) \qquad \langle H \rangle_X = \int_X H(x)dx \; / \int_X dx$$

where H is some function and x might be solid angle, time, or wavelength. Thus increased temporal, spatial, and spectral resolution, will result from decreased integration time, pixel size, and bandpass.

The heterochromatic brightness in magnitudes of solid angle Ω is:

$$(4.1.8) \qquad m(\beta) = m^{(o)}(\beta) - 2.5 \log I(\beta),$$

where $m^{(o)}(\beta)$ is the magnitude zero-point appropriate to bandpass β. Mono- and heterochromatic quantities are:

Spectral Radiances	$L(\lambda),F(\lambda)$	erg/cm^2/sec/ster/A,
Spectral Illumination	$I(\lambda)$	erg/cm^2/sec/A;
Illumination	$I(\beta)$	erg/cm^2/sec,
Power	$P(\beta)$	erg/sec,
Energy	$Q(\beta)$	erg.
Brightness	$m(\beta)$	mag.

§4.2 HETEROCHROMATIC SYSTEM PARAMETERS

Broadband filters deliver heterochromatic measures of the radiant intensity. Thus it is necessary to characterize the incident spectral radiance $L(\lambda)$ and system response $S(\lambda)$ with the help of suitably defined heterochromatic parameters. These may be divided into three categories:

Case (i): The "System Response Solution" gives approximate brightnesses at a precise wavelength λ_o:

λ_o is the Mean Wavelength, precisely defined solely by the System Response $S(\lambda)$. Thus in this case, a precise knowledge of the characteristic wavelength λ_o is offset by uncertainty in brightness.

Case (ii): The "Isophotal Solution" gives precise isophotes at an approximate wavelength λ_i:

λ_i is the Isophotal Wavelength, defined by the condition that energy be precisely conserved. Thus isophotes are precise, despite uncertainty in the wavelength at which energy is conserved.

Case (iii): The "Effective Wavelength Solution" gives approximate brightnesses at an approximate wavelength λ_e:

λ_e is a weighted mean as in case (i), except that in this case the weighting function is the entire radiant throughput $S(\lambda)L(\lambda)$.

Unlike λ_o, both λ_i and λ_e make concessions to the incident spectral radiance. In all cases, uncertainties are necessitated by the broadband nature of the problem. In addition, heterochromatic measures may be weighted either by photon energy (§4.3) or pulse counts (§4.4).

§4.3 ENERGY INTEGRATION

Following equation (4.1.4), let the function:

(4.3.1) $$F(\lambda) = S(\lambda)L(\lambda)$$

be a measure of the spectral radiance delivered by the detector. Since $L(\lambda)$ has units of energy, equation (4.3.1) is the appropriate function for energy-sensitive devices when integrated over wavelength. The heterochromatic radiance F is thus:

(4.3.2) $$F = \int F(\lambda)d\lambda = \int S(\lambda)L(\lambda)d\lambda \ .$$

$S(\lambda)$ is determinable in the laboratory. F is measurable, being the observed radiance weighted by the system response. The functions $L(\lambda)$ and $F(\lambda)$ are generally unknowable through broadband photometry, but it is still possible to gain some knowledge of them by approximate means.

Since $L(\lambda)$ is unknown, it may be approximated by a Taylor expansion about some fiducial wavelength $\hat{\lambda}$:

(4.3.3) $$L(\lambda) = L(\hat{\lambda}) + L'(\hat{\lambda})\ (\lambda-\hat{\lambda}) + L''(\hat{\lambda})\ (\lambda-\hat{\lambda})^2/2! + \ ...$$

where it is assumed that the spectral gradients L', L", ..., are well-behaved. The fiducial wavelength $\hat{\lambda}$ in equation (4.3.3) is free to be chosen so as to facilitate the solution.

One way of generating Cases (i-iii) is as follows:

(i): The more terms retained in equation (4.3.3), the more accurate the representaion of $L(\lambda)$; but $L(\hat{\lambda})$ and its gradients are generally unknown. Nevertheless, the disposable parameter $\hat{\lambda}$ can be chosen to ensure that at least one term of equation (4.3.3) be precisely accounted for; clearly this term should be the one that nullifies the greatest source of uncertainty in the series expansion. Thus if the contribution of the second term in equation

(4.3.3) were to be nullified by a suitable definition of $\hat{\lambda}$, then $L(\lambda)$ will be accurate automatically to 2nd order. The resulting characteristic wavelength λ_o will be an average value of λ weighted by the System Response Function. λ_o is the Mean Wavelength.

(ii): By the Mean Value Theorem, some wavelength λ_i exists such that:

(4.3.4) $$F = L(\lambda_i) \int S(\lambda)\, d\lambda$$

precisely. In this case, only the first term in equation (4.3.3) is retained, but the wavelength $\hat{\lambda} \equiv \lambda_i$ must be sought by approximation through the series expansion. λ_i is the Isophotal Wavelength.

(iii): Alternatively, $\hat{\lambda}$ might be sought by the condition that the Effective Wavelength λ_e be a weighted mean that accounts for both the incident spectral radiance and the losses of the optical path.

These parameters are derived next.

Case (i).

It follows from equations (4.3.2) and (4.3.3) that:

(4.3.5) $$F = L(\hat{\lambda}) \int S(\lambda)d\lambda + L'(\hat{\lambda}) \int S(\lambda)(\lambda-\hat{\lambda})d\lambda + \tfrac{1}{2}L''(\hat{\lambda}) \int S(\lambda)(\lambda-\hat{\lambda})^2 + \ldots$$

Since knowledge of L', L", ... is generally imprecise or lacking, $L(\hat{\lambda})$ will be most accurately determined through the measured quantity F if we specify $\hat{\lambda}$ through the condition:

(4.3.6) $$\int S(\lambda)(\lambda-\hat{\lambda})d\lambda = 0.$$

The quantity λ_o so specified is the Mean Wavelength:

(4.3.7) $$\lambda_o = \int S(\lambda)\lambda d\lambda \;/\; \int S(\lambda)d\lambda \;.$$

Since λ_o is weighted by the Response Function, it lies somewhere in the middle of the range of transmitted radiances. If $S(\lambda)$ is symmetric in λ, then

λ_o coincides with the wavelength of maximum response $S_m(\lambda_m)$. The 3rd term of equation (4.3.5) is a measure of the size of this bandpass; it yields the second order moment:

$$\mu^2(\lambda_o) = \int S(\lambda)(\lambda-\lambda_o)^2 d\lambda \;/\; \int S(\lambda)d\lambda \;. \tag{4.3.8}$$

Higher order moments define the shape of the bandpass.

Substitution of equations (4.3.6) and (4.3.7) in (4.3.5) gives:

$$F = [L(\lambda_o) + \tfrac{1}{2}\mu^2\, L''(\lambda_o) + \ldots] \int S(\lambda)d\lambda \;. \tag{4.3.9}$$

Equations (4.3.7), (4.3.8), and (4.3.9), comprise the System Response Solution to the heterochromatic problem.

Case (ii).

By equation (4.3.4), λ_i must be chosen to ensure that:

$$F = L(\lambda_i) \int S(\lambda)d\lambda \;. \tag{4.3.10}$$

But equation (4.3.9) is also true; thus:

$$L(\lambda_i) = L(\lambda_o) + \tfrac{1}{2}\mu^2\, L''(\lambda_o) + \ldots \tag{4.3.11}$$

Moreover, equation (4.3.3) is also true for any fiducial wavelength, say λ_o. Thus:

$$L(\lambda) = L(\lambda_o) + L'(\lambda_o)(\lambda-\lambda_o) + \tfrac{1}{2}L''(\lambda_o)(\lambda-\lambda_o)^2 + \ldots \tag{4.3.12}$$

Setting $\lambda = \lambda_i$ and comparing equations (4.3.11) and (4.3.12), it follows that the Isophotal Wavelength is:

$$\lambda_i = \lambda_o + \tfrac{1}{2}\mu^2 L''(\lambda_o)/L'(\lambda_o) + \ldots \tag{4.3.13}$$

Equations (4.3.10) and (4.3.13) comprise the Isophotal Wavelength Solution to the heterochromatic problem.

Case (iii).

Instead of equation (4.3.7), the weighting function may be changed to give the Effective Wavelength:

$$\lambda_e = \int \lambda L(\lambda)S(\lambda)d\lambda \; / \; \int L(\lambda)S(\lambda)d\lambda \tag{4.3.14a}$$

$$= \lambda_o + \mu^2 L'(\lambda_o) \; / \; L(\lambda_o) + \ldots \tag{4.3.14b}$$

with the help of equations (4.3.7) and (4.3.12). Equations (4.3.9) and (4.3.14) comprise the Effective Wavelength Solution to the heterochromatic problem. The cases are summarized in Table 4-1.

§4.4 PULSE COUNTING

The photon spectral radiance:

$$N(\lambda) = \lambda L(\lambda)/hc \tag{4.4.1}$$

gives rise to the photon radiant intensity:

$$H = A_e \int N(\lambda)S(\lambda)d\lambda \tag{4.4.2a}$$

$$= (A_e/hc) \int \lambda L(\lambda)S(\lambda)d\lambda, \tag{4.4.2b}$$

where h is Planck's constant and c the speed of light. The function:

$$f = \int N(\lambda)S(\lambda)d\lambda \tag{4.4.3}$$

is the pulse counting analogue of equation (4.3.2). As in equation (4.3.3), $L(\lambda)$ may be expanded in a Taylor series about the fiducial wavelength $\hat{\lambda}$ to give an equation analogous to (4.3.5):

$$f = N(\hat{\lambda}) \int S(\lambda)d\lambda + N'(\hat{\lambda}) \int S(\lambda)(\lambda-\hat{\lambda})d\lambda + \tfrac{1}{2}N''(\hat{\lambda}) \int S(\lambda)(\lambda-\hat{\lambda})^2 d\lambda + \ldots \tag{4.4.4}$$

The arguments of §4.3 for $L(\lambda)$ also apply to $N(\lambda)$. The results are listed in Table 4-2, where the relation (4.4.1) gives:

$$hc\, N(\lambda_o) = \lambda_o\, L(\lambda_o); \tag{4.4.5}$$

$$hc\, N'(\lambda_o) = \lambda_o\, L'(\lambda_o) + L(\lambda_o); \tag{4.4.6}$$

$$hc\, N''(\lambda_o) = \lambda_o\, L''(\lambda_o) + 2\, L'(\lambda_o)\ . \tag{4.4.7}$$

§4.5 FWHM BANDWIDTH

The integrated System Response $\int S(\lambda)d\lambda$ is fundamental to all heterochromatic expressions such as occur in equations (4.3.7) to (4.3.10) and in Tables 4-1 and 4-2. For the sake of simplicity, define S by:

$$\beta S = \int S(\lambda)d\lambda \ , \tag{4.5.1}$$

where:

$$\beta = \lambda_2 - \lambda_1 \tag{4.5.2}$$

is the bandwidth equal to the full width at half maximum (FWHM) of $S(\lambda)$, regardless of weighting. Thus λ_1 and λ_2 are defined by:

$$S(\lambda_1) = S(\lambda_2) = \tfrac{1}{2}S_m(\lambda_m) \tag{4.5.3}$$

where λ_m is the wavelength at which $S(\lambda)$ reaches the maximum S_m. Equation (4.5.1) allows the integrated system response $\int S(\lambda)d\lambda$ to be replaced symbolically by the simpler expression βS.

An approximate formula for β may be derived from the fact that the gradient of $S(\lambda)$ is zero at λ_m. Thus, correct to second order:

$$S(\lambda) = S_m + \tfrac{1}{2}(\lambda-\lambda_m)^2 \, S_m'' + \ldots \tag{4.5.4}$$

Equations (4.5.3) and (4.5.4) give:

$$\lambda_k = \lambda_m \pm (-S_m/S_m'')^{\frac{1}{2}} + \ldots \quad (k=1,2), \tag{4.5.5}$$

so that:

$$\beta = 2(-S_m/S_m'')^{\frac{1}{2}} + \ldots \tag{4.5.6}$$

§4.6 SPECIAL SYSTEM RESPONSES

Square, quadratic, or cubic, responses $S(\lambda)$ $(a<\lambda<b)$ give the following results:

Square:

$$S(\lambda) = K, \quad (a<\lambda<b), \tag{4.6.1a}$$

$$= 0, \quad (a>\lambda>b). \tag{4.6.1b}$$

$$\lambda_o = (b+a)/2, \tag{4.6.2}$$

$$\mu^2 = (b-a)^2/12, \tag{4.6.3}$$

$$\beta = (b-a), \tag{4.6.4}$$

$$S = K. \tag{4.6.5}$$

Quadratic:

$$S(\lambda) = K(\lambda-a)(b-\lambda), \quad (a<\lambda<b). \tag{4.6.6}$$

$$\lambda_o = (b+a)/2, \tag{4.6.7}$$

$$\mu^2 = (b-a)^2/20, \tag{4.6.8}$$

$$\beta = (b-a)/\sqrt{2}, \tag{4.6.9}$$

$$S = K(b-a)^2/3\sqrt{2}. \tag{4.6.10}$$

$S(\lambda)$ is symmetric and the mean wavelength is halfway between the short and long wavelength cutoffs.

Cubic:

$$S(\lambda) = K(\lambda-a)(b-\lambda)(\lambda-c), \quad (a<\lambda<b), \quad (c<a), \tag{4.6.11a}$$

$$= K(\lambda-a)(\lambda-b)(\lambda-c), \quad (a<\lambda<b), \quad (c>a). \tag{4.6.11b}$$

$$\lambda_o = (b+a)/2 - (b-a)^2/20c + \ldots, \quad (|c|>>b), \tag{4.6.12}$$

$$\mu^2 = [1 - (b+a)/2c + \ldots] \, (b-a)^2/20, \quad (|c|>>b). \tag{4.6.13}$$

Exact expressions obtain for all functions in the cubic case, but first order expressions in parameter c show up the effect of skewness in the response. The

mean wavelength is displaced from the halfway mark by an amount that depends on the sign and magnitude of c. In the event that $|c| \to \infty$, the cubic reduces to the quadratic case with appropriate re-definition of K.

Results for asymmetric Poisson or the symmetric Gaussian distribution cannot be expressed in closed form owing to finite (if sometimes small) probabilities of a positive response at "negative" wavelengths; nevertheless the Gaussian case is addressed by Golay (1973), who gives an approximate half-width of 2.36μ about the mean wavelength. This compares to the the exact Gaussian half-width (Bevington 1969) of $\Gamma = 2\sigma\sqrt{2\ln 2} = 2.355\sigma$, where σ is the standard deviation of the distribution.

§4.7 MEAN PIXEL ENERGIES

Equations (4.1.6) and (4.3.1) give:

$$Q_j = A_e \int_T \int_{\omega_j} \int_\lambda F(\lambda)\, dt\, d\omega\, d\lambda \tag{4.7.1}$$

on the assumption that A_e is a constant. The measured energy Q is related to the incident radiance through equation (4.3.2), viz.

$$\int F(\lambda)d\lambda = \int S(\lambda)L(\lambda)d\lambda = F \tag{4.7.2}$$

where F may be chosen from Table 4-1 and equations (4.3.9) and (4.3.10). Thus in cases (i) and (iii):

$$F = [L(\lambda_o) + \tfrac{1}{2}\mu^2\, L''(\lambda_o) + \ldots] \int S(\lambda)d\lambda, \tag{4.7.3}$$

while in case (ii):

$$F = L(\lambda_i) \int S(\lambda)d\lambda. \tag{4.7.4}$$

where the arguments of L are given by equations (4.3.7) or (4.3.13).

In all cases, the ubiquitous integrated system response may be expressed in terms of S and the FWHM bandwidth β according to equation (4.5.1). So equations (4.7.3) and (4.7.4) are more simply written either as:

$$F = \beta\, S\, L(\lambda_o), \tag{4.7.5}$$

[where the argument of L identifies the relevant case (i) or (iii)], or as:

$$F = \beta\, S\, L(\lambda_i) \tag{4.7.6}$$

in case (ii).

On the assumption that β and S are independent of time and direction, equation (4.7.1) becomes:

$$Q_j = A_e\, \beta\, S \int_T \int_{\omega_j} L(\hat{\lambda})\, dt\, d\omega \tag{4.7.7}$$

where the characteristic wavelength $\hat{\lambda}$ is summoned to represent either of the

arguments of L in equations (4.7.5) and (4.7.6).

From Table 4-1, it is clear that $L(\hat{\lambda})$ may depend on one or both of time and direction through one or both of L and $\hat{\lambda}$; i.e. the spectral radiance $L(\lambda)$ may change in intensity or shape over time or direction. Mean values are therefore called for, in the sense of equation (4.1.7). Thus equation (4.7.7) may be written as:

$$Q_j = A_e\ T\ \beta\ S\ \omega_j\ L_j \tag{4.7.8}$$

where it goes without saying that the abbreviated notation L_j represents an average both over time and the solid angle of pixel j, and is to be evaluated according to the prescriptions and wavelengths characteristic of cases (i), (ii), or (iii) [Table 4-1].

The radiance L_j at the aperture of the telescope may arise from the emissivity both of a source "s" as well as an intervening medium "m". Also, the detector "d" itself will contribute to the detected energy. Thus equation (4.7.8) leads to the measured total energy for pixel j:

$$Q_j(s+m+d) = Q_j(s) + Q_j(m) + Q_j(d) \tag{4.7.9a}$$

$$= A_e\ T\ \beta\ S\ \omega_j\ [L_j(s) + L_j(m)] + Q_j(d). \tag{4.7.9b}$$

The radiances L(s) and L(m) are effectively unrelated and are thus linearly additive, and each has its own characteristic wavelength.

Table 4-1.

Optical System Parameters for Energy Integration.

BRIGHTNESSES:

Cases (i), (iii)

$$F = [L(\lambda_o) + \tfrac{1}{2}\mu^2 L''(\lambda_o) + \ldots] \int S(\lambda)d\lambda$$

Case (ii)

$$F = L(\lambda_i) \int S(\lambda)d\lambda$$

WAVELENGTHS:

Case (i)

$$\lambda_o = \int S(\lambda)\lambda d\lambda \;/\; \int S(\lambda)d\lambda$$

$$\mu^2 = \int S(\lambda)(\lambda-\lambda_o)^2 d\lambda \;/\; \int S(\lambda)d\lambda$$

Case (ii)

$$\lambda_i = \lambda_o + \tfrac{1}{2}\mu^2 L''(\lambda_o) \;/\; L'(\lambda_o) + \ldots$$

Case (iii)

$$\lambda_e = \lambda_o + \mu^2 L'(\lambda_o)/L(\lambda_o) + \ldots$$

Table 4-2.

Optical System Parameters for Photon Counting.

BRIGHTNESSES:

Cases (i), (iii)

$$f = [N(\lambda_o) + \tfrac{1}{2}\mu^2 N''(\lambda_o) + \ldots] \int S(\lambda)d\lambda$$

Case (ii)

$$f = N(\lambda_i) \int S(\lambda)d\lambda$$

WAVELENGTHS:

Case (i)

$$\lambda_o = \int S(\lambda)\lambda d\lambda \;/\; \int S(\lambda)d\lambda$$

$$\mu^2 = \int S(\lambda)(\lambda-\lambda_o)^2 d\lambda \;/\; \int S(\lambda)d\lambda$$

Case (ii)

$$\lambda_i = \lambda_o + \tfrac{1}{2}\mu^2 N''(\lambda_o) \;/\; N'(\lambda_o) + \ldots$$

Case (iii)

$$\lambda_e = \lambda_o + \mu^2 N'(\lambda_o)/N(\lambda_o) + \ldots$$

§4.8 DETERMINATION OF SYSTEM RESPONSE

Knowledge of $S(\lambda)$ is basic to radiometry. The energy detected by a laboratory source of known radiance $L(\lambda)$ is given by equations (4.7.1) and (4.7.2), to which must be added a known energy owing to the detector itself. Thus for each pixel j:

$$Q = A_e \int_T \int_{\omega_j} \int_\lambda L(\lambda)\, S(\lambda)\, dt\, d\omega\, d\lambda + Q(d) \,. \tag{4.8.1}$$

Assume that the laboratory radiance is constant and that the pixel is uniformly illuminated by it. Then:

$$\Phi = [Q-Q(d)]/A_e T\omega, \tag{4.8.2}$$

or its equivalent, is a measured and known quantity. Equation (4.8.1) becomes:

$$\Phi = \int L(\lambda)S(\lambda)d\lambda \,. \tag{4.8.3}$$

If $L(\lambda)$ is perfectly monochromatic for all $\lambda = \xi$, then this idealization can be expressed as:

$$L(\lambda) = \delta(\lambda-\xi) \,. \tag{4.8.4}$$

Equation (4.8.3) is then simply:

$$\Phi(\xi) = \int S(\lambda)\ (\lambda-\xi)d\lambda = S(\xi). \tag{4.8.5}$$

On the other hand, with the help of (K+1) radiances:

$$L_i(\lambda_k),\ (i = 0,1,2,\ldots,K)$$

that have sufficiently different gradients, $S(\lambda)$ may be determined at (K+1) spectral points each separated by ε:

$$\lambda = \Lambda + \varepsilon k,\ (k = 0,1,2,\ldots,K). \tag{4.8.6}$$

The short and long wavelength limits are chosen so that $S(\Lambda)$ and $S(\Lambda+\varepsilon K)$ are effectively zero.

By Simpson's Rule:

$$\Phi_i = (\varepsilon/3) \sum_{k=0}^{K} c_k \, L_{i,k}(\lambda_k) S_k(\lambda_k), \tag{4.8.7}$$

where:

$$c_k = \begin{cases} 1, & (k = 0,K) \\ 4, & (k = 1,3,\ldots,K-1) \\ 2, & (k = 2,4,\ldots,K-2). \end{cases} \tag{4.8.8}$$

Let:

$$\Psi_k = (\varepsilon/3) c_k S_k \, . \tag{4.8.9}$$

In matrix notation, equation (4.8.7) becomes:

$$[\Phi] = [L] \cdot [\Psi] \, . \tag{4.8.10}$$

Then:

$$[\Psi] = [L]^{-1} \cdot [\Phi] \tag{4.8.11}$$

gives $S(\lambda)$ at the discrete wavelength intervals of equation (4.8.6) with the help of equations (4.8.8) and (4.8.9). The gradients of the radiances $L(\lambda)$ must differ sufficiently to avoid ill-conditioning.

V. ATMOSPHERIC EXTINCTION

§5.1. MONO- AND HETEROCHROMATIC MAGNITUDES.

The detected heterochromatic radiance F of equations (4.3.2) or (4.7.2) is expressible in terms of monochromatic radiances $L(\lambda)$, where λ may be the mean or isophotal wavelength (Table 4-2). It is desirable to express these quantities in terms of mono- or heterochromatic astronomical magnitudes. In the notation of equations (4.1.4) and (4.5.1), and with the help of equations (4.7.3) and (4.7.4), the detected heterochromatic radiance is:

$$F(\beta) = \int L(\lambda)\, S(\lambda)\, d\lambda \ . \tag{5.1.1}$$

This is:

$$F(\beta) = L(\lambda_o)\, \beta S\, [1 + \tfrac{1}{2}\mu^2\, L''(\lambda_o)/L(\lambda_o) + \ldots], \tag{5.1.2a}$$

in cases (i),(iii), and:

$$F(\beta) = L(\lambda_i)\, \beta S, \tag{5.1.2b}$$

in case (ii) [§4.2].

By equation (4.1.4), the detected heterochromatic illumination of solid angle Ω is:

$$I(\beta,\Omega) = \int F(\beta)\, d\omega \ . \tag{5.1.3}$$

In the sense of equation (4.1.7), suppose $F(\beta,\Omega)$ is an average over solid angle Ω, which is often simply the solid angle subtended by a pixel. Then:

$$I(\beta,\Omega) = \Omega\, F(\beta,\Omega) \ . \tag{5.1.4}$$

By equations (5.1.2a,b), $F(\beta,\Omega)$ is expressible in terms of radiances which are also averages over the pixel; thus:

$$F(\beta,\Omega) = L(\lambda_o,\Omega)\, \beta S\, [1 + \tfrac{1}{2}\mu^2\, L''(\lambda_o,\Omega)/L(\lambda_o,\Omega) + \ldots], \tag{5.1.5a}$$

in cases (i),(iii), and:

$$F(\beta,\Omega) = L(\lambda_i,\Omega)\, \beta S, \tag{5.1.5b}$$

in case (ii).

Thus heterochromatic magnitudes corresponding to the pixel solid angle may be calculated from measured or known quantities. By equation (4.1.8):

(5.1.6) $\quad m(\beta,\Omega) = m^{(o)}(\beta) - 2.5 \log I(\beta,\Omega).$

Since:

(5.1.7) $\quad \log(1+x) = \log e\ (x + \ldots),\ (x<<1),$

equations (5.1.4) - (5.1.6) give:

$$m(\beta,\Omega) - m^{(o)}(\beta)$$

(5.1.8a) $$= -2.5\ [\log L(\lambda_o,\Omega) + \log\Omega\beta S + \log e\ \tfrac{1}{2}\mu^2 L''(\lambda_o,\Omega)/L(\lambda_o,\Omega) + \ldots],$$

(5.1.8b) $$= -2.5\ [\log L(\lambda_i,\Omega) + \log\Omega\beta S].$$

in the various cases (i)-(iii). In this way, measured illumination is expressed in magnitudes.

Evidently, it should be possible to estimate monochromatic magnitudes at the mean and isophotal wavelengths from the heterochromatic magnitudes of equations (5.1.8a,b). Let the spectral illumination incident upon the objective of the telescope be:

(5.1.9) $\quad J(\lambda,\Omega) = \int L(\lambda)\ d\omega .$

Again in the sense of equation (4.1.7), this is:

(5.1.10) $\quad J(\lambda,\Omega) = \Omega\ L(\lambda,\Omega)\ .$

Define monochromatic magnitudes at the telescope objective, and over Ω, to be:

(5.1.11) $\quad m(\lambda,\Omega) - m^{(o)}(\lambda) = -2.5 \log J(\lambda,\Omega),$

where $m^{(o)}(\lambda)$ is the magnitude zero-point corresponding to wavelength λ. Let λ be either λ_o or λ_i; then equations (5.1.10) and (5.1.11) enable $L(\lambda_o,\Omega)$ or $L(\lambda_i,\Omega)$ to be eliminated from equations (5.1.8a,b). Thus:

$$m(\beta,\Omega) - m^{(o)}(\beta)$$

(5.1.12a) $$= m(\lambda_o,\Omega) - m^{(o)}(\lambda_o) - 2.5[\log\beta S + \log e\ \tfrac{1}{2}\mu^2 L''(\lambda_o,\Omega)/L(\lambda_o,\Omega) + \ldots],$$

(5.1.12b) $$= m(\lambda_i,\Omega) - m^{(o)}(\lambda_i) - 2.5 \log\beta S\ .$$

§5.2. MONOCHROMATIC MAGNITUDE RELATIONS

The relation between $m(\lambda_o)$ and $m(\lambda_i)$ follows directly from equations (5.1.12a) and (5.1.12b):

$$m(\lambda_i) - m^{(o)}(\lambda_i)$$
$$= m(\lambda_o) - m^{(o)}(\lambda_o) - 2.5 \log_e \tfrac{1}{2}\mu^2 L''(\lambda_o)/L(\lambda_o) + \ldots \tag{5.2.1}$$

where for notational simplicity the argument of solid angle is suppressed. To find the corresponding relation for the effective wavelength λ_e, use the expansion $\lambda L(\lambda) = \lambda_e L(\lambda_e) + (\lambda-\lambda_e)[L(\lambda_e) + \lambda_e L'(\lambda_e)] + \ldots$ to get:

$$\int \lambda L(\lambda) S(\lambda) d\lambda = \lambda_e L(\lambda_e) \int S(\lambda) d\lambda + [L(\lambda_e) + \lambda_e L'(\lambda_e)] \int (\lambda-\lambda_e) S(\lambda) d\lambda + \ldots$$

By definitions (4.3.6) and (4.5.1), $\int (\lambda-\lambda_e) S(\lambda) d\lambda = (\lambda_o-\lambda_e)\beta S$, so that:

$$\int \lambda L(\lambda) S(\lambda) d\lambda = [\lambda_e L(\lambda_e) + \{L(\lambda_e) + \lambda_e L'(\lambda_e)\}(\lambda_o-\lambda_e)]\beta S + \ldots$$

Substitution of this into the definition (4.3.14a) of λ_e, gives:

$$\int L(\lambda) S(\lambda) d\lambda = L(\lambda_e)[1+\{L(\lambda_e)+\lambda_e L'(\lambda_e)\}(\lambda_o-\lambda_e)/\lambda_e L(\lambda_e)+\ldots]\beta S.$$

But by equations (4.3.2) and (4.3.4), the left-hand side is just $L(\lambda_i)\beta S$. So:

$$L(\lambda_i) = L(\lambda_e)\,[1 + \{1 + \lambda_e L'(\lambda_e)/L(\lambda_e)\}\{(\lambda_o/\lambda_e)-1\} + \ldots]. \tag{5.2.2}$$

Conversion to magnitudes is accomplished by using equations (5.1.10) and (5.1.11), and the approximation (5.1.7) gives:

$$m(\lambda_i) - m^{(o)}(\lambda_i)$$
$$= m(\lambda_e) - m^{(o)}(\lambda_e) - 2.5 \log_e[(\lambda_o/\lambda_e)-1][1+\lambda_e L'(\lambda_e)/L(\lambda_e)] + \ldots \tag{5.2.3}$$

Nevertheless, it is desirable to express all monochromatic magnitudes in terms of quantities that depend only on λ_o. By equation (4.3.14b):

$$1 - \lambda_o/\lambda_e = \mu^2 L'(\lambda_o)/\lambda_o L(\lambda_o) + \ldots .$$

Also $L(\lambda_e) = L(\lambda_o) + (\lambda_e-\lambda_o)L'(\lambda_o) + \ldots$, and $L'(\lambda_e) = L'(\lambda_o) + \ldots$. Further reduction gives:

$$m(\lambda_e) - m^{(o)}(\lambda_e)$$
$$= m(\lambda_o) - m^{(o)}(\lambda_o)$$
$$-1.25 \log_e \mu^2 \,[L''(\lambda_o)/L(\lambda_o)+2L'(\lambda_o)/\lambda_o L(\lambda_o)+2\{L'(\lambda_o)/L(\lambda_o)\}^2]. \tag{5.2.4}$$

§5.3. MONOCHROMATIC EXTINCTION.

The rule by which monochromatic radiance is diminished by the atmosphere is simply:

(5.3.1) $$L(\lambda,z) = L_o(\lambda)\ \exp[-k(\lambda)M(z)].$$

Here and henceforth, subscripts "o" denotes values outside the atmosphere; $k(\lambda)$ is the monochromatic extinction coefficient; and $M(z)$ signifies the relative air mass at zenith angle z in units of the air mass at the zenith. For many practical purposes:

(5.3.2) $$M(z) = \sec z$$

to an accuracy of 1% up to $z = 65°$; more accurate values are tabulated by Schoenberg (1929), and may be calculated from Bemporad's formula:

(5.3.3) $$M(z) = \sec z - a_1(\sec z - 1) - a_2(\sec z - 1)^2 - a_3(\sec z - 1)^3 ,$$

where a_i (i=1,2,3) are small coefficients (Hardie 1962). Equation (5.3.3) is valid to $z = 80°$ with an accuracy of perhaps 1%.

Generalize the definition (5.1.11) to cover unextinguished monochromatic magnitudes:

(5.3.4) $$m_o(\lambda,\Omega) - m^{(o)}(\lambda) = -2.5 \log \Omega L_o(\lambda,\Omega).$$

Similarly, for extinguished magnitudes:

(5.3.5) $$m(\lambda,\Omega,z) - m^{(o)}(\lambda) = -2.5 \log \Omega L(\lambda,\Omega,z)$$
$$= -2.5 \log \Omega L_o(\lambda,\Omega)\exp[-k(\lambda)M(z)].$$

In particular, λ may be either the mean or isophotal wavelength. Subtraction and suppression of the argument Ω gives:

(5.3.6) $$m(\lambda,z) = m_o(\lambda) + 2.5\log e\ k(\lambda)M(z)$$

with $2.5\log e = 1.086$. This and equation (5.3.1) is the Lambert-Bouguer Law; its simplicity tempts photometrists to seek a similar relation for heterochromatic extinction, but the wider the bandpass the more corrections are required.

§5.4. BANDPASS EFFECTS ON EXTINCTION.

The heterochromatic magnitude $m(\beta,\Omega)$ of equation (5.1.6) corresponds to a detected illumination over solid angle Ω and bandpass β; in the case of atmospheric extinction, it should be rewritten as:

(5.4.1) $$m(\beta,\Omega,z) - m^{(o)}(\beta) = -2.5 \log I(\beta,\Omega,z),$$

in order to signify that $I(\beta,\Omega,z)$ is detected when the telescope points at an angle z from the zenith. The definition of I must be modified to account for zenith angle. By equations (5.1.3) and (5.1.4), we let:

(5.4.2) $$I(\beta,\Omega,z) = \int F(\beta,z)\, d\omega = \Omega\, F(\beta,z)\ ,$$

where as before we are concerned with radiances averaged over the smallest resolution element. Thus with the help of equation (5.1.2a) [cases (i) and (iii)], the extinguished illumination is:

(5.4.3) $$I(\beta,\Omega,z) = L(\lambda_o,z)\ \Omega\beta S\ [1 + \tfrac{1}{2}\mu^2 L''(\lambda_o,z)/L(\lambda_o,z) + \ldots],$$

while in case (ii):

(5.4.4) $$I(\beta,\Omega,z) = L(\lambda_1,z)\ \Omega\beta S\ .$$

In equation (5.4.3), the approximation in square brackets involves the detected monochromatic radiance and its second derivative evaluated at λ_o.

With the help of equation (5.3.5), the extinguished monochromatic radiance $L(\lambda_o,z)$ or $L(\lambda_1,z)$ in equations (5.4.3) or (5.4.4) may be expressed readily in terms of the monochromatic extinction coefficient $k(\lambda_o)$ or $k(\lambda_1)$ respectively. However in the case of equation (5.4.3), the heterochromatic illumination is also dependent on the 2^{nd} derivative of the detected radiance $L(\lambda_o,z)$; and this 2^{nd} derivative will in turn entail knowledge of the 2^{nd} derivative of $k(\lambda_o)$ as well as $L''(\lambda_o)$.

By use of equations (5.3.1), (5.4.3), and (5.1.7), equation (5.4.1) becomes:

$$(5.4.5)\qquad m(\beta,\Omega,z) - m^{(o)}(\beta)$$
$$= -2.5 \log \beta S - 2.5 \log [\Omega L(\lambda_o)]$$
$$-2.5\log e \tfrac{1}{2}\mu^2 \frac{d^2}{d\lambda_o^2}\{L_o(\lambda_o)e^{-k(\lambda_o)M(z)}\}/L_o(\lambda_o)\, e^{-k(\lambda_o)M(z)} + \ldots$$

But equation (5.3.5) can eliminate the second term in favor of extinguished monochromatic magnitudes at the mean wavelength. It follows that:

$$(5.4.6)\qquad m(\beta,\Omega,z) - m^{(o)}(\beta)$$
$$= m(\lambda_o,\Omega,z) - m^{(o)}(\lambda_o) - 2.5 \log \beta S$$
$$-2.5\log e \tfrac{1}{2}\mu^2 \frac{d^2}{d\lambda_o^2}\{L_o(\lambda_o)e^{-k(\lambda_o)M(z)}\}/L_o(\lambda_o)\, e^{-k(\lambda_o)M(z)} + \ldots$$

In the event that there is no air mass, $M(z) \equiv 0$, and equation (5.4.6) becomes:

$$(5.4.7)\qquad m_o(\beta,\Omega) - m^{(o)}(\beta)$$
$$= m_o(\lambda_o,\Omega) - m^{(o)}(\lambda_o) - 2.5\log\beta S$$
$$-2.5\log e \tfrac{1}{2}\mu^2\, L_o''(\lambda_o)/L_o(\lambda_o) + \ldots$$

Again, the argument of solid angle may be omitted in equations (5.4.6) and (5.4.7), bearing in mind that it is implied for magnitudes so calculated. On subtracting equations (5.4.6) and (5.4.7), the magnitude zero-points and the bandwidth-sensitivity factor βS fall away as they should. The heterochromatic extinction correction $m(\beta,z) - m_o(\beta)$ is then expressible in terms of the monochromatic extinction correction $m(\lambda_o,z) - m(\lambda_o)$, which in turn is given by the equation (5.3.6). Thus:

$$(5.4.8)\quad m(\beta,z) - m_o(\beta) = 2.5 \log e\, k(\lambda_o)M(z)$$
$$-2.5\log e \tfrac{1}{2}\mu^2 \frac{d^2}{d\lambda_o^2}\{L_o(\lambda_o)e^{-k(\lambda_o)M(z)}\}/L_o(\lambda_o)\, e^{-k(\lambda_o)M(z)} + \ldots$$
$$+2.5\log e \tfrac{1}{2}\mu^2\, L_o''(\lambda_o)/L_o(\lambda_o) + \ldots$$

Equation (5.4.8) reduces to (5.3.6) only for narrow-band photometry (i.e. μ negligibly small).

Inspection of equation (5.4.8) shows that the term containing $L_o''(\lambda_o)/L_o(\lambda_o)$ cancels, but the term containing $L_o'(\lambda_o)/L_o(\lambda_o)$ does not. Let:

$$(5.4.9)\qquad L_o'(\lambda_o)/L_o(\lambda_o) = \ln 10\ d\log L_o(\lambda_o)/d\lambda_o$$
$$= \ln 10\ [\log L_o(\lambda_o^+) - \log L_o(\lambda_o)]/[\lambda_o^+ - \lambda_o] + \ldots$$

where $\lambda_o^+ > \lambda_o$ by the conventional use of forward differences. But by equation (5.4.5), the difference in the logarithms of L_o at the two mean wavelengths may be expressed in terms of the difference in the heterochromatic magnitudes at these mean wavelengths; leading terms only need to be considered in this approximation. Thus equation (5.4.9) leads to:

$$(5.4.10)\qquad 2.5\ L_o'(\lambda_o)/L_o(\lambda_o)$$
$$= \ln 10\ [m_o(\beta) - m_o(\beta^+) - m^{(o)}(\beta) + m^{(o)}(\beta^+) - 2.5 \log(\beta^+ S^+/\beta S)]/[\lambda_o^+ - \lambda_o]$$
$$+ \ldots$$

where:

$$(5.4.11)\qquad m_o(\beta) - m_o(\beta^+) = \Gamma_o(\beta, \beta^+)$$

is a color index outside the atmosphere. The approximations (5.4.9) and (5.4.10) assume that the mean wavelengths λ_o^+ and λ_o corresponding to bandpasses β^+ and β are not too far apart.

The required differentiations in equation (5.4.8) give the leading terms of the appropriate heterochromatic extinction law in terms of color index Γ, bandpass sensitivity factors βS, magnitude zero-points, and $k(\lambda_o)$ and its derivatives $k'(\lambda_o)$ and $k''(\lambda_o)$. With the help of equation (5.4.10), the law is:

$$(5.4.11)\qquad m(\beta, z) - m_o(\beta)$$
$$= [k_1(\beta) + k_2(\beta)\Gamma_o(\beta, \beta^+)]M(z) + k_3(\beta)M^2(z) + \ldots$$

in which the new extinction coefficients are now labelled appropriately in broadband notation. They are:

(5.4.12a) $$k_1(\beta) = 2.5\log_e k(\lambda_o) + 2.5\log_e \tfrac{1}{2}\mu^2 k''(\lambda_o) + k_2(\beta)\,[m^{(o)}(\beta^+) - m^{(o)}(\beta) + 2.5\,\log(\beta S/\beta^+ S^+)],$$

(5.4.12b) $$k_2(\beta) = \mu^2 k'(\lambda_o)/(\lambda_o^+ - \lambda_o),$$

(5.4.12c) $$-k_3(\beta) = 1.25\,\log_e\,[\mu(\lambda_o)k'(\lambda_o)]^2.$$

The leading term in the estimation of heterochromatic extinction would still obey Bouger's law were it not for terms in the color index and a quadratic term in air mass. Conditions for neglect of these terms is derived in the next section.

§5.5. CONDITIONS FOR NEGLECT OF TERMS.

It is instructive to estimate the various contributions to each extinction coefficient $k_i(\beta)$ (i=1,2,3) in equations (5.4.12a-c). For illustrative purposes, choose the Johnson UBV system (Johnson 1966), whose system parameters are listed in the first three columns of Table 5-1. In addition, estimates for $k(\beta)$ and its derivatives are needed. For this purpose, a surprisingly accurate fit to monochromatic extinction is:

(5.5.1) $$k(\lambda) = 0.24\ (0.447/\lambda)^3.$$

All wavelengths are measured in microns. Equation (5.5.1) is a quasi-Rayleigh scattering law, and supplies the last three columns of Table 5-1, which are used to derive the values in Table 5-2.

The second and third columns of Table 5-2 account for the first two terms in $k_1(\beta)$ [equation (5.4.12a)]. In all cases, the dominant term is still the monochromatic extinction $1.087k(\lambda_o)$; the second term in equation (5.4.12a) is 1½ orders of magnitude less, while the last term of $k_1(\beta)$ is even smaller (since both the zero-point magnitude difference of the Johnson system, and the logarithm of the relative bandpass-sensitivities, are small).

The fourth column of Table 5-2 gives the term $k_2(\beta)$ which multiplies the color index:

(5.5.2) $$\Gamma_o(\beta,\beta^+) = (U-B)_o \text{ or } (B-V)_o$$

in the forward difference convention of equation (5.4.9). The values listed show that the color index contribution is more than an order of magnitude smaller than the leading term in $k_1(\beta)$, thereby warranting the label "second order extinction coefficient".

The last column of Table 5-2 gives the term multiplying the square of the relative air mass; the smallness of $k_3(\beta)$ may be deceptive, since the product $k_3(\beta)M^2(z)$ may be significant at large air masses.

An absolute criterion for the neglect of the color index term is that:

(5.5.3) $$|k_2(\beta)\Gamma_o M(z)| \leq \varepsilon \ .$$

For purposes of estimation, take M(z) = sec z [equation (5.3.2)]. Thus:

(5.5.4) $$|\Gamma_o| \leq \varepsilon \cos z \ / \ k_2(\beta),$$

Table 5-3 gives the ranges of permissible color indices U-B and B-V [equation (5.5.2)], for ε=0.01 (appropriate for 1% photometry), as a function of zenith angle z. It is seen that the smaller the zenith distance z, the greater the latitude of color indices that permit neglect of the second order color term; and in theory, only color indices close to zero are permitted down to the horizon.

The absolute condition for neglect of the quadratic air mass correction is:

(5.5.5) $$k_3(\beta)\ M^2(z) \leq \varepsilon,$$

or:

(5.5.6) $$\sec z \leq \sqrt{\varepsilon/k_3(\beta)} \ .$$

Table 5-4 gives ranges of zenith angle z over which the term may be neglected, for 1% or 2% photometry in U or B. Curvature in the Bouger-type linear relation is expected for observations that extend beyond these limits.

Table 5-1.
System parameters and monochromatic extinction terms for the Johnson UBV photometric system.

	μ^2	$(\mu/\lambda_o)^2$	λ_o	$k(\lambda_o)$	$k'(\lambda_o)$	$k''(\lambda_o)$
U	4.6×10^{-4}	3.76×10^{-3}	0.350	0.50	-4.3	49
B	1.3×10^{-3}	6.53×10^{-3}	0.477	0.24	-1.6	14
V	1.6×10^{-3}	5.22×10^{-3}	0.556	0.13	-0.67	4.8

Table 5-2.
Component contributions to heterochromatic extinction.

	λ_o	$1.087k(\lambda_o)$	$0.543\mu^2k''(\lambda_o)$	$k_2(\beta)$	$k_3(\beta)$
U	0.350	0.54	0.012	0.020	-0.0046
B	0.477	0.26	0.010	0.019	-0.0018
V	0.556	0.14	0.0042	-	-0.0004

Table 5-3.
Ranges of permissible Color Indices for 1% photometry.

z	0°	10°	20°	30°	40°	50°	60°	70°	80°
$\pm(U-B)_o$	0.50	0.49	0.47	0.43	0.38	0.32	0.25	0.17	0.09
$\pm(B-V)_o$	0.53	0.52	0.49	0.46	0.40	0.34	0.26	0.18	0.09

Table 5-4.
Ranges of permissible zenith distance for photometry in U and B.

ε	0.01	0.02
$z(U) \leq$	47°	61°
$z(B) \leq$	65°	73°

§5.6. EFFECTIVE WAVELENGTH CORRECTION.

The results of §5.4 et seq. pertain to case (i) (§4.2 and Table 4-1). In the event that magnitudes are required at the effective wavelength λ_e [case (iii)], it is seen from Table 4-1 that the previously derived magnitudes are unchanged, but λ_e must be calculated from equation (4.3.14), viz.

$$\lambda_e = \lambda_o + \mu^2\, L'(\lambda_o)/L(\lambda_o) + \ldots\ .$$

This expression must now be rewritten to account for extinction.

At the detector:

$$\lambda_e(z) = \lambda_o + \mu^2\, L'(\lambda_o,z)/L(\lambda_o,z) + \ldots\ , \tag{5.6.1}$$

whereas at the top of the atmosphere:

$$\lambda_{e,o} = \lambda_o + \mu^2\, L_o'(\lambda_o)/L_o(\lambda_o) + \ldots\ . \tag{5.6.2}$$

The difference between equations (5.6.1) and (5.6.2) gives the correction that must be applied to find the extra-atmospheric effective wavelength:

$$\lambda_{e,o}-\lambda_e(z) = \mu^2[L_o'(\lambda_o)/L_o(\lambda_o)-L'(\lambda_o,z)/L(\lambda_o,z)] + \ldots\ . \tag{5.6.3}$$

The monochromatic extinction law (5.3.1) gives the difference of the ratios:

$$L_o'(\lambda_o)/L_o(\lambda_o)-L'(\lambda_o,z)/L(\lambda_o,z) = k'(\lambda_o)\, M(z), \tag{5.6.4}$$

and it follows that the effective wavelength correction can be written in a remarkably tidy form:

$$\lambda_{e,o}-\lambda_e(z) = \mu^2\, k'(\lambda_o)\, M(z)\ . \tag{5.6.5}$$

By equation (5.4.12b), the correction may be expressed in terms of the second order heterochromatic extinction coefficient:

$$\lambda_{e,o}-\lambda_e(z) = (\lambda_o^{+}-\lambda_o)\, k_2(\beta)\, M(z)\ . \tag{5.6.6}$$

Equations (5.6.5) and (5.6.6) imply that 2-color photometry is necessary to derive the effective wavelength correction. The value of the correction may be

estimated for the Johnson UBV system with the help of Table 5-2; given that $k_2(\beta) \cong 0.02$, and that $(\lambda_o^+ - \lambda_o) \sim 0.1$, the correction is $\sim 0.002\ M(z)$, and in fact need not be applied at air masses less than about 5 ($z \sim 78°$) in order to achieve an accuracy of 1%.

The extra-atmospheric effective wavelength may be derived directly from equation (5.6.2), with the help of equations (5.4.10) and (5.4.11):

(5.6.7)

$$\lambda_{e,o} = \lambda_o + 0.41\ln 10\ \mu^2\ [\Gamma_o(\beta,\beta_o^+) - m^{(o)}(\beta) - m^{(o)}(\beta_o^+) - 2.5\log(\beta^+ S^+/\beta S)]/(\lambda_o^+ - \lambda_o) + \ldots\ .$$

It would seem reasonable to write an analogous equation for the observed effective wavelength:

(5.6.8)

$$\lambda_e(z) = \lambda_o + 0.41\ln 10\ \mu^2\ [\Gamma(\beta,\beta_o^+) - m^{(o)}(\beta) - m^{(o)}(\beta_o^+) - 2.5\log(\beta^+ S^+/\beta S)]/(\lambda_o^+ - \lambda_o) + \ldots\ .$$

The difference between (5.6.7) and (5.6.8) is simply:

(5.6.9) $$\lambda_{e,o} - \lambda_e(z) = 0.41\ln 10\ \mu^2\ [\Gamma_o(\beta^+,\beta) - \Gamma(\beta^+,\beta)]/(\lambda_o^+ - \lambda_o),$$

which at first glance seems to bear little resemblance to equation (5.6.6). However, with the help of the definition (5.4.11) of color index Γ, this difference becomes:

(5.6.10) $$\lambda_{e,o} - \lambda_e(z) = 0.41\ln 10\ \mu^2\ [k_1(\beta^+)M(z) + \ldots + k_3(\beta^+)M^2(z) - k_1(\beta)M(z) - \ldots - k_3(\beta)M^2(z)]/(\lambda_o^+ - \lambda_o),$$

in which leading terms only are retained (i.e. the second order chromatic terms are justifiably neglected). The terms in k_3 can be neglected too provided:

(5.6.11) $$M(z) \leq \varepsilon \left| k_1(\beta)/k_3(\beta) \right|$$

Equation (5.6.11) for neglect of the term in $M^2(z)$ differs from the criterion (5.5.5) inasmuch as it is a relative (not an absolute) criterion. Moreover, since equation (5.6.10) is already of second order, it is reasonable to take ε to be 10%. Then from Table 5-2, M(z) must be less than about 12 in the worst case.

Thus equation (5.6.10) becomes:

(5.6.11) $$\lambda_{e,o} - \lambda_e(z) = 0.4 \ln 10 \; \mu^2 \; M(z) \; [k_1(\beta^+) - k_1(\beta)]/(\lambda_o^+ - \lambda_o),$$

which can be written:

(5.6.12) $$\lambda_{e,o} - \lambda_e(z) = \mu^2 \; M(z) \; [k(\lambda_o^+) - k(\lambda_o)]/(\lambda_o^+ - \lambda_o),$$

with the help of equation (2.4.12a). Equations (5.6.5) and (5.6.12) are one and the same to first order.

VI. SURFACE BRIGHTNESS FROM STANDARD STARS.

§6.1. Radiative Transfer

If the Earth's atmosphere extinguishes light, it must also emit light. Let κ_ν and j_ν be the mass extinction and emission coefficients at density ρ in the atmosphere. If the optical depth τ_ν of the atmosphere increases along the direction of an incoming light ray, then:

$$d\tau_\nu = - \kappa_\nu \rho \, ds \, , \tag{6.1.1}$$

where the pathlength s is measured outward. An incoming ray of radiance L_ν at frequency ν is governed by the equation of radiative transfer (Goody 1964):

$$- \frac{dL_\nu}{d\tau_\nu} = L_\nu - S_\nu \, , \tag{6.1.2}$$

where:

$$S_\nu = j_\nu / \kappa_\nu \tag{6.1.3}$$

is the source function.

The integrating factor $\exp(\tau_\nu)$ enables a formal solution to equation (6.1.2) to be found:

$$L_\nu(\tau_\nu) = L_\nu(0)\exp(-\tau_\nu) + \int_0^{\tau_\nu} S_\nu(\tau'_\nu) \exp(-\tau_\nu+\tau'_\nu) \, d\tau'_\nu \, . \tag{6.1.4}$$

The first term in equation (6.1.4) is simply the Bouguer-Lambert Law (5.3.1), according to which the incoming radiance $L_\nu(0)$ at the top of the atmosphere is attenuated by $\exp(-\tau_\nu)$ by the time it reaches the telescope. When the source function is not negligible, the Bouguer-Lambert term must be augmented by the second term, which accounts for atmospheric emissivity from all points along the line of sight. The source function is attenuated over the optical thickness from the source to the telescope, and integrated over all sources to the top of the atmosphere.

If the source function were to depend solely on the radiance imposed at the top of the atmosphere, then equation (6.1.4) would be an integral equation for L_ν. In the present case, S_ν is completely dominated by other sources, whose net effect is to provide illumination to the night sky. Equation (6.1.4) can then be written as the sum of the attenuated radiance of a source "*" observed at zenith distance z through an optical thickness $\tau_\nu(z)$, and the contribution from the sky "s":

$$L_\nu(z) = L_{\nu,o}(*)\ \exp[-\tau_\nu(z)] + L_\nu(z,s). \tag{6.1.5}$$

§6.2. Detected Energies.

Consider a detector that is energy cumulative, and consider each term of equation (6.1.5) in turn.

(a) Celestial Sources.

The energy arising from a source "*" of attenuated radiance $L(\lambda,z;*)$ seen at zenith distance z is to be found from the first term of equation (6.1.5). Following equation (4.1.6), the attenuated starlight supplies an energy to solid angle ω_j of pixel j through a bandpass β at zenith distance z, of:

$$Q_j(\beta,\omega_j,z;*) = \int_{A_e}\int_{T}\int_{\omega_j}\int_{\beta} S(\lambda)\, L(\lambda,z;*)\, d\lambda\, d\omega\, dt\, da\ .$$

Assume that the integrand is independent of areal effects; then:

$$Q_j(\beta,\omega_j,z;*) = A_e \int_{T}\int_{\omega_j}\int_{\beta} S(\lambda)\, L(\lambda,z;*)\, d\lambda\, d\omega\, dt\ . \tag{6.2.1}$$

By equation (5.1.1), the detected heterochromatic radiance of the attenuated starlight is:

$$F(\beta,z;*) = \int_{\beta} S(\lambda)\, L(\lambda,z;*)\, d\lambda\ , \tag{6.2.2}$$

so that equation (6.2.1) becomes:

$$Q_j(\beta,\omega_j,z;*) = A_e \int_{T}\int_{\omega_j} F(\beta,z;*)\, d\omega\, dt\ . \tag{6.2.3}$$

By equation (5.4.2), the detected illumination of the attenuated starlight is:

$$I(\beta,\omega_j,z;*) = \int_{\omega_j} F(\beta,z;*)\, d\omega\ , \tag{6.2.4}$$

so that equation (6.2.3) becomes:

$$Q_j(\beta,\omega_j,z;*) = A_e \int_{T} I(\beta,\omega_j,z;*)\, dt\ . \tag{6.2.5}$$

By equation (5.4.1), which is adapted from equation (4.1.8), the illumination

is expressed in apparent magnitudes over the solid angle ω_j as:

$$I(\beta,\omega_j,z;*) = 10^{-0.4[m(\beta,\omega_j,z;*) - m^{(o)}(\beta)]} . \tag{6.2.6}$$

Consequently, equation (5.2.5) is:

$$Q_j(\beta,\omega_j,z;*) = A_e \int_T 10^{-0.4[m(\beta,\omega_j,z;*) - m^{(o)}(\beta)]} dt . \tag{6.2.7}$$

The detected energy can be expressed in terms of magnitudes outside the atmosphere by use of equation (5.4.11); the argument of solid angle was suppressed there, and may now be reinstated, to give:

$$Q_j(\beta,\omega_j,z;*) = A_e \int_T 10^{-0.4[m_o(\beta,\omega_j;*)-m^{(o)}(\beta)+\{k_1(\beta)+k_2(\beta)\Gamma(\beta,\beta^+,\omega_j)\}M(z)+k_3(\beta)M^2(z)]} dt. \tag{6.2.8}$$

Note that the argument of m_o in equation (6.2.8) clearly implies that m_o is the unattenuated magnitude merely of that part of an image that happens to fall in the pixel solid angle ω_j. Thus if the source is a star, m_o would equal the unattenuated star magnitude either when the pixel solid angle is large enough to accomodate the attenuated (and therefore blurred) image, or if many pixels are used to cover the image. The former case presents no further complication.

In the latter case, summation over a sufficient number of pixels, say:

$$j = 1,2,\ldots,J , \tag{6.2.9}$$

must occur in order to ensure that all of the attenuated energy is accumulated. In the case of stars, their apparent sizes have been discussed by Young (1974), from which the value of J may be derived. Let:

$$\Omega = \sum_{j=1}^{J} \omega_j , \tag{6.2.10}$$

be the solid angle, generously configured to encompass the image. As a result,

equations (6.2.8) and (6.2.10) lead to:

(6.2.11)

$$Q(\beta,\Omega,z;*) = \sum_{j=1}^{J} Q_j(\beta,\omega_j;z)$$

$$= A_e \sum_{j=1}^{J} \int_T 10^{-0.4[m_o(\beta,\omega_j;*)-m^{(o)}(\beta)+\{k_1(\beta)+k_2(\beta)\Gamma(\beta,\beta^+,\omega_j)\}M(z)+k_3(\beta)M^2(z)]} .$$

A further property of equations (6.2.8) and (6.2.11) is noteworthy. Factors in the integrand arising from the first two terms of the exponent are (or may) be constant in time, but the terms in air mass M(z) are generally not because z is a function of time. Moreover, even at a given instant, M(z) varies across a pixel or a star image. Therefore make the assumptions (whose bounds of validity will be discussed later):

(6.2.12a) The integration time T is sufficiently brief that a mean air mass can replace M(z) in equation (6.2.11).

and:

(6.2.12b) Air mass varies insignificantly across pixels and star images.

Without further ado, equation (6.2.8) becomes:

(6.2.13)

$$Q_j(\beta,\omega_j,z;*) = A_e\, T\, 10^{-0.4[m_o(\beta,\omega_j;*)-m^{(o)}(\beta)+\{k_1(\beta)+k_2(\beta)\Gamma(\beta,\beta^+,\omega_j)\}M(z)+k_3(\beta)M^2(z)]} ,$$

while equation (6.2.11) becomes:

(6.2.14)

$$Q(\beta,\Omega,z;*) = \sum_{j=1}^{J} Q_j(\beta,\omega_j,z;*)$$

$$= A_e\, T\, 10^{-0.4[m_o(\beta,\Omega;*)-m^{(o)}(\beta)+\{k_1(\beta)+k_2(\beta)\Gamma(\beta,\beta^+,\Omega)\}M(z)+k_3(\beta)M^2(z)]} .$$

Equation (6.2.14) is a summation over j of the preceding equation, and so it must be possible to relate the magnitudes occurring in both. Taking the ratio in light of assumption (6.2.12b), it follows that:

$$(6.2.15) \qquad Q(\beta,\Omega,z;*)/Q(\beta,\omega_j,z;*) = 10^{-0.4[m_o(\beta,\Omega;*)-m_o(\beta,\omega_j;*)]},$$

in which the z-dependence is redundant given the cancellation of extinction corrections. In fact, a similar quotient may be formed from equation (6.2.6) and its analogue in Ω, so equation (6.2.15) holds for apparent magnitudes as well.

In reality, (6.2.15) is a flexible equation describing the relation between magnitudes detected by different solid angles. Only the solid angle arguments need retained in an obvious notation:

$$(6.2.16) \qquad Q(\Omega;*)/Q_j(\omega_j;*) = 10^{-0.4[m(\Omega;*)-m(\omega_j;*)]}.$$

With the help of equations (6.2.6) and (6.2.4), the quotient is:

$$(6.2.17) \qquad 10^{-0.4[m(\Omega;*)-m(\omega_j;*)]} = \int_{\Omega} F(\omega;*)d\omega \; / \; \int_{\omega_j} F(\omega;*)d\omega \; .$$

Suppose Ω comprises J pixels of size ω_j. By analogy with equation (6.2.10), the numerator can be written:

$$(6.2.18) \qquad \int_{\Omega} F(\omega;*)d\omega = \sum_{j=1}^{J} \int_{\omega_j} F(\omega;*)d\omega \; .$$

With a resolution of ω_j one can do no better than to let $\Phi_j(*)$ be an average for the pixel. Then:

$$(6.2.19) \qquad \int_{\omega_j} F(\omega;*)d\omega = \Phi_j(*)\ \omega_j \; .$$

The quotient (6.2.16) becomes:

$$(6.2.20) \qquad Q(\Omega;*)/Q_j(\omega_j;*) = \sum_{j=1}^{J} \omega_j\ \Phi_j(*) \; / \; \omega_j\ \Phi_j(*) \; .$$

If a source has a uniform surface brightness, then all $\Phi_j(*)$'s are equal, and:

$$(6.2.21) \qquad \begin{aligned} Q(\Omega;*)/Q_j(\omega_j;*) &= 10^{-0.4[m(\Omega;*)-m(\omega_j;*)]}, \\ &= \Omega/\omega_j \; . \end{aligned}$$

This could also have been derived from equation (5.1.6). Thus for example, if "*" denotes the sky "s" of uniform surface brightness, 10 pixels are 2.5 mag brighter than 1 pixel.

(b) The Sky.

Similar arguments pertain to the derivation of energies deposited by the sky. By ana logy with equation (6.2.7):

$$Q_j(\beta,\omega_j,z;s) = A_e \int_T 10^{-0.4[m(\beta,\omega_j,z;s) - m^{(o)}(\beta)]}\, dt \,. \tag{6.2.22}$$

There is no need to allow for extinction, since this is already accounted for by the transfer solution (6.1.5). Again invoking assumptions (6.2.12a,b), equation (6.2.22) gives an equation analogous to (6.2.13):

$$Q_j(\beta,\omega_j,z;s) = A_e\, T\, 10^{-0.4[m(\beta,\omega_j,z;s)-m^{(o)}(\beta)]} \,. \tag{6.2.23}$$

If attenuated stellar energy over solid angle Ω is recorded in addition, then equation (6.2.23) must be summed over all relevant pixels:

$$Q(\beta,\Omega,z;s) = A_e\, T \sum_{j=1}^{J} 10^{-0.4[m(\beta,\omega_j,z;s)-m^{(o)}(\beta)]} \,. \tag{6.2.24}$$

(c) Detector.

In general, the detector "d" supplies power $P_j(\omega_j;d)$ to each pixel. The total energy accumulated by each pixel over integration time T is:

$$Q_j(\omega_j;d) = \int_T P_j(\omega_j;d)\, dt \,, \tag{6.2.25}$$

while over solid angle Ω the integrated energy is:

$$Q(\Omega;d) = \sum_{j=1}^{J} \int_T P_j(\omega_j;d)\, dt \,. \tag{6.2.26}$$

This quantity is regarded as known.

The energy contribution (6.2.25) from the detector (that integrates in bandpass β) can be expressed in equivalent magnitudes $m(\omega_j;d)$:

$$Q_j(\omega_j;d) = A_e T\, 10^{-0.4[m(\omega_j;d)-m^{(o)}(\beta)]} . \tag{6.2.27}$$

$Q_j(\omega_j;d)/A_e T$ has the units of illumination as required by the definition of magnitude, and is determinable under conditions of no incident light. For solid angle Ω, the integrated dark current of the detector provides energy:

$$Q(\Omega;d) = A_e T \sum_{j=1}^{J} 10^{-0.4[m(\omega_j;d)-m^{(o)}(\beta)]} , \tag{6.2.28}$$

which must be the same as that in equation (6.2.27) if $\omega_j = \Omega$ there; i.e.:

$$Q(\Omega;d) = A_e T\, 10^{-0.4[m(\Omega;d)-m^{(o)}(\beta)]} . \tag{6.2.29}$$

Equations (6.2.28) and (6.2.29) (and others) also provide the rule:

$$10^{-0.4\, m(\Omega)} = \sum_{j=1}^{J} 10^{-0.4\, m(\omega_j)} . \tag{6.2.30}$$

§6.3 Formal Extinction Solutions.

The difference:

(6.3.1) $$Q_j(\beta,\omega_j,z;*) = Q_j(\beta,\omega_j,z;*+s+d) - Q_j(\beta,\omega_j,z;s) - Q_j(\omega_j;d) ,$$

gives the attenuated energy of "*" alone, and this in turn is a function of the extinction coefficients by equation (6.2.13). However, $Q_j(\beta,\omega_j,z;s)$ cannot be measured in the direction of "*". The standard way around this problem is to measure the sky in the vicinity of "*" and to strike a suitable average.

Assume that:

(6.3.2) pixels can be located near the source whose brightness equals that of the sky in the direction of the source.

Denote such a pixel by the subscript j'; its energy is:

(6.3.3) $$Q_{j'}(\beta,\omega_{j'},z;s+d) = Q_{j'}(\beta,\omega_{j'},z;s) + Q_{j'}(\omega_{j'};d) .$$

By assumption (6.3.2):

(6.3.4) $$Q_{j'}(\beta,\omega_{j'},z;s) = Q_j(\beta,\omega_j,z;s) ,$$

but generally:

(6.3.5) $$Q_{j'}(\omega_{j'};d) \neq Q_j(\omega_j;d) .$$

Equation (6.3.3) is therefore:

(6.3.6) $$Q_{j'}(\beta,\omega_{j'},z;s+d) = Q_j(\beta,\omega_j,z;s) + Q_{j'}(\omega_{j'};d) .$$

Equations (6.3.6) and (6.3.1) give:

(6.3.7) $$Q_j(\beta,\omega_j,z;*) = Q_j(\beta,\omega_j,z;*+s+d)-Q_{j'}(\beta,\omega_{j'},z;s+d)-\{Q_j(\omega_j;d)-Q_{j'}(\omega_{j'};d)\}.$$

Quantities on the r.h.s. are now all potentially knowable; represent them by the difference:

(6.3.8) $$\Delta Q_{jj'}(\beta,\omega_j,\omega_{j'},z;*) = Q_j(\beta,\omega_j,z;*+s+d)-Q_{j'}(\beta,\omega_{j'},z;s+d)-\{Q_j(\omega_j;d)-Q_{j'}(\omega_{j'};d)\}.$$
$$= Q_j(\beta,\omega_j,z;*).$$

Comparison of equations (6.2.13) and (6.3.8) gives:

$$(6.3.9)\qquad (1/A_eT)\ 10^{+0.4[m_o(\beta,\omega_j;*)-m^{(o)}(\beta)]}\ \Delta Q_{jj'}(\beta,\omega_j,\omega_{j'},z;*) = 10^{-0.4[\{k_1(\beta)+k_2(\beta)\Gamma_{o,j}(\beta,\beta^+,\omega_j)\}M(z)+k_3(\beta)M^2(z)]},$$

$$(j = 1,2,\ldots,J).$$

$M(z)$, Γ_j, and quantities on the l.h.s. of equation (6.3.9), are knowable when pixel j records energy from a source of known magnitude and color. The color index subscript j and argument ω_j allows temporarily for the possibility that the source is intrinsically extended; it will be dropped for sources that are extrinsically extended (i.e. blurred by seeing). Also, the arguments of $\Delta Q_{jj'}$ make it clear that z in M(z) is appropriate to each j. Difficulty in choosing pixel j' diminishes the usefulness of standard sources of large angular extent. Resolved standard sources are more likely to be galaxies or nebulae of small angular extent, and as such will be governed by the theory for point sources.

For standard stars, the exponential on the r.h.s. of equation (6.3.9) may be taken to the r.h.s. and the equation summed over J to give:

$$(6.3.10)\qquad (1/A_eT)\ 10^{+0.4[m_o(\beta,\Omega;*)-m^{(o)}(\beta)]}\ \Delta Q(\beta,\Omega,\Omega',z;*) = 10^{-0.4[\{k_1(\beta)+k_2(\beta)\Gamma_o(\beta,\beta^+)\}M(z)+k_3(\beta)M^2(z)]}.$$

where summation of equation (6.3.8) has given:

$$(6.3.11)\qquad \Delta Q(\beta,\Omega,\Omega',z;*) = Q(\beta,\Omega,z;*+s+d)-Q'(\beta,\Omega',z;s+d)-\{Q(\Omega;d)-Q'(\Omega';d)\}.$$

$$= Q(\beta,\Omega,z;*)\ .$$

m_o and Γ_o in equation (6.3.10) are now the unattenuated magnitude and color index of a star seen through relative air mass M(z). If these and $\Delta Q(z;*)$ are

known, the three unknown extinction coefficients on the r.h.s. require at least three such stars for their determination.

Let subscripts:

(6.3.12) $\qquad i = 1,2,\ldots,I\ ,$

denote I standard stars at zenith distances z_i. Insert subscript i in equations (6.3.10) and (6.3.11), and let $Z_i(z_i)$ be -2.5 times the logarithm of the r.h.s. of equation (6.3.10):

(6.3.13) $\quad Z_i(z_i)$

$$= -2.5 \log \left[(1/A_e T)\ 10^{+0.4[m_{o,i}(\beta,\Omega_i;*)-m^{(o)}(\beta)]}\ \Delta Q_i(\beta,\Omega_i,\Omega',z_i;*)\right]$$

$$= -\,m_{o,i}(\beta,\Omega_i;*) + m^{(o)}(\beta) - 2.5 \log \left[\Delta Q_i(\beta,\Omega_i,\Omega',z_i;*)/A_e T\right]\ .$$

Thus equation (6.3.10) becomes:

(6.3.14) $\quad Z_i(z_i) = \left\{k_1(\beta)+k_2(\beta)\Gamma_{o,i}(\beta,\beta^+)\right\}M(z_i)+k_3(\beta)M^2(z_i),\ (i = 1,2,\ldots,I).$

If $M(z_i)$ is regarded as known via equations (5.3.2) or (5.3.3), then this is a system of I simultaneous non-homogeneous linear algebraic equations in the 3 unknown extinction coefficients $k_\ell(\beta)$, $\ell = 1,2,3$.

A minimum condition for the solution of equations (6.3.14) is that I = 3; but this condition is only necessary, and not sufficient, as the following case demonstrates. Let I = 3 stars have the same zenith angle z. Subtract the I^{th} equation from those with i = 1 and 2. System (6.3.14) is then:

(6.3.15) $\quad Z_i(z) = k_2(\beta)\ M(z)\ \left\{\Gamma_{o,i}(\beta,\beta+) - \Gamma_{o,3}(\beta,\beta^+)\right\}\ ,\ i = 1,2.$

Only the secondary extinction coefficient can be found, and then only if the color indices of stars i = 1,2 are sufficiently different from the third; the extinction coefficient k_1 which accounts for most of the extinction, goes undetermined. This leads to the important result: a necessary and sufficient minimum condition for the solution of the 3 extinction coefficients is that there be 3 standard stars with different zenith angles and color indices.

In practice, it is necessary to overdetermine the system (6.3.14) by use of I >> 3 standard stars having a large range of colors, and to proceed by use of least squares. Since $M(z_i)$ is common to all terms on the r.h.s. of equation (6.3.14), and is assumed to be known, the system to be solved may be written as:

(6.3.16) $$Z_i(z_i)/M(z_i) = k_1(\beta)+k_2(\beta)\Gamma_{o,i}(\beta,\beta^+)+k_3(\beta)M(z_i),\ (i = 1,2,\ldots,I).$$

§6.4. Zenith Angle and Color Index Ranges.

A result of §6.3 is that a range of z is necessary for the solution of of the primary extinction coefficient k_1 in system (6.3.14), whereas a range of Γ is necessary for the solution of the secondary color coefficient k_2. Moreover, the tertiary coefficient waits to assert itself at large z. Such effects represent competing claims to significance, and thus to numerical accuracy. To guage the situation in a preliminary way, consider the following arguments.

The range of color index affects only k_2, whereas the range in air mass M(z) is common to all terms in equation (6.3.14). Thus, let:

$$z_i = \bar{z} \pm \delta z_i \ , \tag{6.4.1}$$

where $\bar{z}$ is a zenith angle somewhere in the middle of the range of the I stars, and $2|\delta z_i| <$ F.O.V. (the field of view of the detector). To evaluate the sizes of the competing claims, it suffices to take M(z) = sec z. Then:

$$M(z_i) = \sec(\bar{z} \pm \delta z_i), \tag{6.4.2}$$

which can be written:

$$M(z_i) = M(\bar{z}) \left\{1 \pm f_i(\bar{z}, \delta z_i)\right\} . \tag{6.4.3}$$

To a first approximation, let:

$$M(\bar{z}) = \sec \bar{z} \ , \tag{6.4.4}$$

so that the function f_i is exactly:

$$f_i(\bar{z}, \delta z_i) = (\cos \delta z_i - \tan \bar{z} \sin \delta z_i)^{-1} - 1. \tag{6.4.5}$$

Values of f_i are listed in Table 6-1. In particular:

$$f_i(\bar{z}, 0) = 0, \tag{6.4.6}$$

and:

$$f_i(0, \delta z_i) = \sec \delta z_i - 1 \ . \tag{6.4.7}$$

Choose $\bar{z}$ to be the zenith distance of the I^{th} star, so that $\delta z_I = f_I(\bar{z}, 0) = 0$. Applying equation (6.3.14) gives:

Table 6-1

The function $f(\bar{z},\delta z) \times 10^2$.

δz \ $\bar{z}$	0°	10°	20°	30°	40°	50°
½°	0.00	0.16	0.32	0.51	0.74	1.05
1°	0.02	0.32	0.65	1.03	1.50	2.14
2°	0.06	0.68	1.35	2.12	3.08	4.41

δz \ $\bar{z}$	60°	70°	75°	80°	85°	87°
½°	1.54	2.46	3.37	5.21	11.1	20.0
1°	3.13	5.05	6.98	11.0	24.9	50.0
2°	6.50	10.7	15.1	24.8	66.5	200.

(6.4.8) $$Z_i(z_i) - Z_I(z_I)$$
$$= \pm k_1 M(\bar{z}) f_i + k_2 M(\bar{z})[(1\pm f_i)\Gamma_{o,i} - \Gamma_{o,I}] + k_3 M^2(\bar{z})(\pm 2f_i + f_i^2).$$

When $f_i = 0$, the case pertaining to equation (6.3.15) is recovered (i.e. the primary coefficient can be found only if there is a range in z). But $|f_i|$ must then not be too large lest it be swamped by the tertiary contributions. Generally it would be desirable to have:

(6.4.9) $$k_1 \geq |k_3 M(\bar{z})| \; | \; 2\pm f_i \; |.$$

By Table 5-2, $|k_3|$ is two orders of magnitude less than k_1 in the Johnson system, so $| \; 2\pm f_i \; | \leq 100 \cos\bar{z}$ or:

(6.4.10) $$2 - 100 \cos \bar{z} < |f_i| < 2 + 100 \cos \bar{z} \; .$$

The more stringent inequality on the l.h.s (for stars closer than average to the horizon) gives the absolute limit of no permissible range in z: cosz = 0.02 for an elevation angle of 1°10'. Only narrow ranges of z are permissible if bandpass effects beyond μ^2 are neglected, whereas near the zenith, large ranges are allowed [and are desirable in fact, according to equation (6.3.15)].

Competing requirements on ranges of z and color are evident in the second term of equation (6.4.8). Consider the conditions on the first and second terms of (6.4.8), viz. that (i) the second term doesn't dominate the first, and conversely (ii) the first doesn't dominate the second. For want of a number, write these respectively as:

(6.4.11) $$k_1|f_i| \geq |k_2[(1\pm f_i)\Gamma_i - \Gamma_I]| \geq k_1|f_i|/100.$$

By Table 5-2, k_2 is an order of magnitude less than k_1, so that:

(6.4.12) $$10|f_i| \geq |(\Gamma_i - \Gamma_I) \pm f_i\Gamma_i| \geq |f_i|/10 \; .$$

Consider two cases:

(a) if $|f_i|$ is small compared to $|\Gamma_i - \Gamma_I|$ then:

(6.4.13) $$10|f_i| \geq |\Gamma_i - \Gamma_I| \geq |f_i|/10 \; .$$

The case of equation (6.3.15) is implicit in the first inequality, which states also that a small range of z restricts the simultaneous solution for the primary and color coefficients. The second inequality states that the range of color index differences must exceed a certain fraction of $|f_i|$ in order for the second term to be determinable to a given accuracy.

(b) if $|f_i|$ is large compared to $|\Gamma_i - \Gamma_I|$, then:

(6.4.14) $$10 \geq |\Gamma_i| \geq 1/10 ,$$

which is reasonable.

§6.5. Apparent Magnitudes.

To describe the appearance of a pixel in magnitudes $m(\beta,\omega_j,z;*+s)$, it is necessary to subtract detector energies $Q(\omega_j;d)$ from total energies $Q(\beta,\omega_j,z;*+s+d)$; i.e.:

$$Q(\beta,\omega_j,z;*+s+d)-Q(\omega_j;d) = A_e T\, 10^{-0.4[m(\beta,\omega_j,z;*+s)-m^{(o)}(\beta)]}. \tag{6.5.1}$$

With the help of equation (6.3.8), this can be expressed in terms of $\Delta Q(*)$:

$$A_e T\, 10^{-0.4[m(\beta,\omega_j,z;*+s)-m^{(o)}(\beta)]} = \Delta Q(\beta,\omega_j,\omega_{j'},z;*+s+d) + Q'(\beta,\omega_{j'},z;s+d) - Q'(\omega_{j'};d). \tag{6.5.2}$$

The appearance of the source follows from summation over J:

$$A_e T\, 10^{-0.4[m(\beta,\Omega,z;*+s)-m^{(o)}(\beta)]} = Q(\beta,\Omega,z;*+s+d) - Q(\Omega;d) = \Delta Q(\beta,\Omega,\Omega',z;*+s+d) + Q'(\beta,\Omega',z;s+d) - Q'(\Omega';d). \tag{6.5.3}$$

In particular, if "*" contributes nothing to the differences in equations (6.5.1) and (6.5.2), then the apparent magnitude of the sky follows from:

$$A_e T\, 10^{-0.4[m(\beta,\omega_j,z;s)-m^{(o)}(\beta)]} = Q'(\beta,\omega_{j'},z;s+d) - Q'(\omega_{j'};d). \tag{6.5.4}$$

More reliable statistics for sky brightness in the vicinity of a star result from summation over J:

$$A_e T\, 10^{-0.4[m(\beta,\Omega,z;s)-m^{(o)}(\beta)]} = Q'(\beta,\Omega',z;s+d) - Q'(\Omega';d). \tag{6.5.5}$$

Equation (6.2.30) may be used to reduce sky brightness to convenient units (e.g. mag/arcsec^2).

§6.6 Derived Magnitudes.

In equation (6.3.13), let subscript "u" connote a source whose unattenuated magnitude is unknown. Then by writing the color index explicitly according to equation (5.5.2), the unattenuated magnitude in bandpass β is:

$$(6.6.1)\qquad m_{o,u}(\beta,\Omega,{*u}) = m^{(o)}(\beta) - 2.5\log[\Delta Q(\beta,\Omega,\Omega',z_u;{*u})/A_eT] - k_1(\beta)M(z_u) - k_2(\beta)M(z_u)[m_{o,u}(\beta)-m_{o,u}(\beta^+)] - k_3(\beta)M^2(z_u)\ .$$

The extinction coefficients can be determined from I>>3 standard stars, and only the forward component in bandpass β^+ of the color index $[m_{o,u}(\beta)-m_{o,u}(\beta^+)]$ remains to be determined. To get $m_{o,u}(\beta^+)$ requires a second solution in β^+ from a second exposure of time T^+ and zenith angles z^+; thus:

$$(6.6.2)\qquad m_{o,u}(\beta^+,\Omega,{*u}) = m^{(o)}(\beta^+) - 2.5\log[\Delta Q(\beta^+,\Omega,\Omega',z_u^+;{*u})/A_eT^+] - k_1(\beta^+)M(z_u^+) - k_2(\beta^+)M(z_u^+)[m_{o,u}(\beta^+)-m_{o,u}(\beta^{++})] - k_3(\beta^+)M^2(z_u^+)\ .$$

The need for $m_{o,u}(\beta^+)$ in equation (6.6.1) arises only in the second order color coefficient, and thus only first order terms in equation (6.6.2) are necessary. Thus replace $m_{o,u}(\beta^+)$ in equation (6.6.1) by:

$$(6.6.3)\qquad m_{o,u}(\beta^+) = m^{(o)}(\beta^+) - 2.5\log[\Delta Q(\beta^+,\Omega,\Omega',z_u^+;{*u})/A_eT^+] - k_3(\beta^+)M^2(z_u^+)\ ,$$

where the tertiary coefficient term is retained lest it be significant. Thus $m_{o,u}(\beta,\Omega,{*u})$ can be determined.

To determine the unattenuated color index of the source, the difference between equations (6.6.1) and (6.6.2) is necessary; but to get $m_{o,u}(\beta^+,\Omega,{*u})$, it is necessary to know the next forward magnitude $m_{o,u}(\beta^{+++})$. This may be found in the same way from a third solution in bandpass β^{+++}. Thus in the Johnson U,B,V system for example, unattenuated magnitudes (U,B) and color

indices (U-B,B-V) can be found. Then magnitude:

(6.6.4) $$V = B - (B-V)$$

follows.

Instead of using the forward convention of equation (5.4.9), backward differences could also be used, in which case the analysis of equations (5.4.9) to (5.4.12) must be reworked. Then the backward difference equivalent of equation (6.6.4) would be: U = B + (U-B). It is noteworthy that the heterochromatic coefficients $k_1(\beta)$ and $k_2(\beta)$ would then be slightly different, as seen from equations (5.4.12a,b). Presumably, the magnitudes obtained by forward differences would be the same as those found by backward differences to the accuracy retained in the analysis.

Equations (6.6.1) to (6.6.3) obtain equally for pixel solid angles ω_j. Thus unattenuated surface brightnesses and colors of extended sources can be obtained for each pixel, and reduced to convenient units (mags/arcsec^2) with the help of equation (6.2.21).

VII. DETECTOR CALIBRATION.

§7.1 Analog Devices.

Energies Q appearing from equations (4.1.6) to (6.6.3) are required in digital form in order for solutions to be found, yet often are recorded by analog devices. Such devices are usually not precisely linear; an extreme example is the photographic emulsion, though in both CCD and photographic photometry the approach to saturation manifests itself as a curvature in the response.

In general, the energy deposited on pixel j may be expressed as a function of a dimensionless parameter D that measures the analog output:

$$Q_j = Q_j(D_j) \ . \tag{7.1.1}$$

In the case of photography, D would be the specular photographic density. Following the work of Zou, Chen, and Peterson (1981), let the function $Q_j(D_j)$ be modeled by a polynomial series:

$$Q_j = \sum_{n=1}^{N} C_n^{(o)} \, P_{n,j}(D_j;p) \ , \tag{7.1.2}$$

where parameter N is assigned and p is an optimization parameter that minimizes the discrepancy between observed and derived magnitudes of the standard stars for the assigned N. Note specifically that the coefficients $C_n^{(o)}$ in equation (7.1.2) have units of energy. In the case of photography, the polynomial P may be the standard rectification function of Baker (1925) and Sampson (1925) raised to the power (np):

$$P_{n,j}(D_j;p) = [10^{D_j} - 1]^{np} \ . \tag{7.1.3}$$

Wherever energy Q has appeared in the foregoing sections, it may be replaced by the development (7.1.2). The relevant notation signifies the conditions that obtain; thus for example, subscript j and argument "s+d" imply

that $D_j(s+d)$ is the analog output for pixel j for sky plus detector. To relieve notational overload, the bandpass arguments will be dropped.

Thus from equation (6.3.8) it follows that:

$$\Delta Q_{jj'}(\omega_j,\omega_{j'},z;*) \tag{7.1.4}$$

$$= \sum_{n=1}^{N} C_n^{(o)} \left[P_{n,j}\{D_j(*+s+d);p\} - P_{n,j'}\{D_{j'}(s+d);p\}\right.$$

$$\left. - P_{n,j}\{D_j(d);p\} + P_{n,j'}\{D_{j'}(d);p\}\right].$$

However by equation (6.3.9), this is:

$$A_e T\ 10^{-0.4[m_o(\omega_j;*) - m^{(o)} + k_1 M(z) + k_2 M(z)\Gamma_o + k_3 M^2(z)]} \tag{7.1.5}$$

$$= \sum_{n=1}^{N} C_n^{(o)} \left[P_{n,j}\{D_j(*+s+d);p\} - P_{n,j'}\{D_{j'}(s+d);p\}\right.$$

$$\left. - P_{n,j}\{D_j(d);p\} + P_{n,j'}\{D_{j'}(d);p\}\right]$$

Since coefficients $C_n^{(o)}$ are to be determined, they might as well be replaced by:

$$C_n = (1/A_e T)\ 10^{-0.4m^{(o)}}\ C_n^{(o)}\ . \tag{7.1.6}$$

Thus the effective collecting area is absorbed into determinable coefficients; its value need not be known, but what is required is that:

(7.1.7) A_e is the same wherever a solution is to be applied.

Note that this limitation imposes a further constraint on the range of zenith angles (cf. §6.4).

Equation (7.1.5) becomes therefore:

$$10^{-0.4\ [m_o(\omega_j;*) + k_1 M(z) + k_2 M(z)\Gamma_o + k_3 M^2(z)]} \tag{7.1.8}$$

$$= \sum_{n=1}^{N} C_n \left[P_{n,j}\{D_j(*+s+d);p\} - P_{n,j'}\{D_{j'}(s+d);p\}\right.$$

$$\left. - P_{n,j}\{D_j(d);p\} + P_{n,j'}\{D_{j'}(d);p\}\right].$$

Summing over j yields an expression for the known magnitude $m_{o,i}(*)$ of star i:

$$10^{-0.4\,[m_{o,i}(*) + k_1 M(z_i) + k_2 M(z_i)\Gamma_{o,i} + k_3 M^2(z_i)]} \tag{7.1.9}$$

$$= \sum_{n=1}^{N} C_n \sum_{j,j'=1}^{J} [P_{n,j,i}\{D_{j,i}(*+s+d);p\} - P_{n,j',i}\{D_{j',i}(s+d);p\}$$

$$- P_{n,j,i}\{D_{j,i}(d);p\} + P_{n,j',i}\{D_{j',i}(d);p\}]$$

$$(i = 1,2,\ldots,I).$$

This is a nonlinear system of equations that permits solution for the three extinction ceofficients and the N calibration coefficients.

Equation (7.1.9) is the denoument of the foregoing analysis. Amongst other things, it shows that ground-based detector calibration cannot be accomplished by use of standard stars unless extinction coefficients are simultaneously part of the solution. This principle has previously been asserted (Usher 1986), but is here spelled out in complete detail, along with implicit assumptions. In addition, the apparent disappearance of the magnitude zero-point in the work of Zou et al., is clarified, as is the role of the effective collecting area.

Moreover, the sky brightness will now emerge as a derived quantity, whose value also cannot be found without a concomitant solution for extinction; again, this principle is in accord with the equation of radiative transfer and its solution (6.1.5). From equation (6.5.4):

$$10^{-0.4m(\omega_{j'},z;s)} = \sum_{n=1}^{N} C_n\,[P_{n,j'}\{D_{j'}(s+d);p\} - P_{n,j'}\{D_{j'}(d);p\}], \tag{7.1.10}$$

or from equation (6.5.5):

$$10^{-0.4m(\Omega',z;s)} = \sum_{n=1}^{N} C_n \sum_{j'=1}^{J} [P_{n,j'}\{Dj'(s+d);p\} - P_{n,j'}\{D_{j'}(d);p\}]. \tag{7.1.11}$$

The appearance of pixels (i.e. with detector noise subtracted) is found from equation (6.5.1):

$$10^{-0.4m(\omega_j,z;\hat{s}^{*+})} = \sum_{n=1}^{N} C_n \left[P_{n,j}\{D_j(*+s+d);p\} - P_{n,j}\{D_j(d);p\}\right]. \tag{7.1.12}$$

The apparent (attenuated) magnitude of a star i (i.e. with sky and detector noise subtracted) follows from equations (7.1.9) and (5.4.11):

$$10^{-0.4\ m_i(z_i;*)} = \sum_{n=1}^{N} C_n \sum_{j,j'=1}^{J} \left[P_{n,j,i}\{D_{j,i}(*+s+d);p\} - P_{n,j',i}\{D_{j',i}(s+d);p\} - P_{n,j,i}\{D_{j,i}(d);p\} + P_{n,j',i}\{D_{j',i}(d);p\}\right]. \tag{7.1.13}$$

§7.2 Perturbation Iteration.

Given the complexity of non-linear multivariate analysis, it seems reasonable to attempt a solution to equation (7.1.9) by linearization and iteration, using Newton's method. Let:

(7.2.1)

$$\Delta P_{i,n}(p) = \sum_{j,j'=1}^{J} [P_{n,j,i}\{D_{j,i}(*+s+d);p\} - P_{n,j',i}\{D_{j',i}(s+d);p\} - P_{n,j,i}\{D_{j,i}(d);p\} + P_{n,j',i}\{D_{j',i}(d);p\}],$$

so that equation (7.1.9) is (with self-evident notational economy):

$$(7.2.2) \quad 10^{-0.4[m_i+k_1M_i+k_2M_i\Gamma_i+k_3M_i^2]} = \sum_{n=1}^{N} \Delta P_{i,n}(p)\, C_n \ , \ (i = 1,2,\ldots I).$$

Perturbation of both sets of coefficients gives:

$$(7.2.3a) \qquad k_\ell = k_\ell^{(c)} + \delta k_\ell \ , \ (\ell = 1,2,3),$$

$$(7.2.3b) \qquad C_n = C_n^{(c)} + \delta C_n \ , \ (n = 1,2,\ldots,N),$$

where superscript (c) signifies a value initially guessed or subsequently corrected during the iteration process. Values for $k_\ell^{(c)}$ can be estimated from Table 5-2 with fair accuracy; corresponding values of $C_n^{(c)}$ can be found by solving equation (7.2.2), which is for this purpose a linear regression problem. Corrections δk_ℓ and δC_n are therefore small, so that to first order:

$$(7.2.4) \qquad 10^x = 1 + (\ln 10)\, x + \ldots \ .$$

Corrections δk_ℓ and δC_n will be governed by the following linearized system, derived by substituting equations (7.2.3a,b) into equation (7.2.2), using equation (7.2.4), and retaining first order terms:

(7.2.5)

$$0.4\ln 10\, M_i(\delta k_1+\Gamma_i\delta k_2+M_i\delta k_3)+10^{0.4[m_i+k_1^{(c)}M_i+k_2^{(c)}\Gamma_iM_i+k_3^{(c)}M_i^2]} \cdot \sum_{n=1}^{N} \Delta P_{i,n}(p)\, \delta C_n$$

$$= 1 - 10^{0.4[m_i+k_1^{(c)}M_i+k_2^{(c)}\Gamma_iM_i+k_3^{(c)}M_i^2]} \cdot \sum_{n=1}^{N} \Delta P_{i,n}(p)\, C_n^{(c)} \ .$$

Equation (7.2.5) is now an overdetermined linear system of the form:

$$A\,X = Y \,, \tag{7.2.6}$$

whose solution is (Bates and Watts 1988):

$$X = (A^T A)^{-1} A^T Y \,. \tag{7.2.7}$$

"T" signifies a transposed matrix. Specifically:

$$X = \left| \delta k_1 \quad \delta k_2 \quad \delta k_3 \quad \delta C_1 \quad \delta C_2 \ldots \delta C_N \right|^T , \tag{7.2.8}$$

$$A = \begin{vmatrix} 0.41n10\ M_1 & .. & 0.41n10\ M_1^2 & \Delta P_{11}(p) & \ldots & \Delta P_{1N}(p) \\ 0.41n10\ M_2 & .. & 0.41n10\ M_2^2 & \Delta P_{21}(p) & \ldots & \Delta P_{2N}(p) \\ . & . & . & . & . & . \\ 0.41n10\ M_I & .. & 0.41n10\ M_I^2 & \Delta P_{I1}(p) & \ldots & \Delta P_{IN}(p) \end{vmatrix} , \tag{7.2.9}$$

and:

$$Y = \begin{vmatrix} 1-10^{0.4[m_1+k_1^{(c)}M_1+k_2^{(c)}\Gamma_1 M_1+k_3^{(c)}M_1^2]} \cdot \sum_{n=1}^{N} \Delta P_{1n}(p) C_n^{(c)} \\ 1-10^{0.4[m_2+k_1^{(c)}M_2+k_2^{(c)}\Gamma_2 M_2+k_3^{(c)}M_2^2]} \cdot \sum_{n=1}^{N} \Delta P_{2n}(p) C_n^{(c)} \\ . \\ 1-10^{0.4[m_I+k_1^{(c)}M_I+k_2^{(c)}\Gamma_I M_I+k_3^{(c)}M_I^2]} \cdot \sum_{n=1}^{N} \Delta P_{In}(p) C_n^{(c)} \end{vmatrix} . \tag{7.2.10}$$

Iterative solutions progress to the point where vector X gives no improvement in the corrected coefficients, whereupon successive completed iterations give the residual sum-of-squares function of p:

$$S(p) = \sum_{i=1}^{I} Y_i^2(p) \,. \tag{7.2.11}$$

Comparison of equations (7.2.10) and (7.2.2) shows that a best solution to the nonlinear regression is achieved when S(p) is a minimum. Thus p is determined for a given N and used in subsequent calculations.

§7.3 Air Mass as Unknown.

In §7.1 and §7.2, it is assumed that the relative air mass M(z) is a known function (5.3.2) or (5.3.3) of secant z. However the secant law is a consequence of the assumption of plane parallelism, and may start to fail at larger zenith angles (§5.3), even though the law is still a fairly good approximation.

The actual dependence M(z) may be found as part of the solution of the nonlinear least squares problem (7.1.9), by perturbing M(z) as well as the extinction and polynomial coefficients; thus in addition to equations (7.2.3a,b), let:

$$M_i(z_i) = M_i^{(c)}(z_i) + \delta M_i(z_i), \qquad (i=1,2,\ldots,I), \tag{7.3.1}$$

where the initial guess $M_i^{(c)}$ might be found from equation (5.3.2). Regarding $M_i(z_i)$ as an unknown for every star i implies that there will always be (N+3) more unknowns than there are standard stars for their determination. In practice, corrections M_i will be virtually the same within observational error for stars within a particular range of zenith angle; this range might even encompass the entire field of view. Let there be:

$$m = 1,2,\ldots,M \tag{7.3.2}$$

ranges of zenith angle for which a solution is sought, and:

$$i = 1,2,\ldots,I_m \tag{7.3.3}$$

stars in each range, so that the sum total of available standards is still:

$$I = I_1 + I_2 + \ldots + I_m \ . \tag{7.3.4}$$

The statistical analog of Newton's Method can then be applied to each band of zenith angle.

Retention of first order perturbed terms gives the generalization of equation (7.2.5):

(7.3.5)

$$0.4\ln 10[\delta k_1 M_m^{(c)}+\delta k_2 \Gamma_i M_m^{(c)}+\delta k_3\{M_m^{(c)}\}^2+\delta M_m\{k_1^{(c)}+\Gamma_i k_2^{(c)}+2k_3^{(c)}\}]$$

$$+ 10^{0.4[m_i+k_1^{(c)}M_m^{(c)}+k_2^{(c)}\Gamma_i M_m^{(c)}+k_3^{(c)}\{M_m^{(c)}\}^2]} \cdot \sum_{n=1}^{N} \Delta P_{i,n}(p)\ \delta C_n$$

$$= 1 - 10^{0.4[m_i+k_1^{(c)}M_m^{(c)}+k_2^{(c)}\Gamma_i M_m^{(c)}+k_3^{(c)}\{M_m^{(c)}\}^2]} \cdot \sum_{n=1}^{N} \Delta P_{i,n}(p)\ C_n\ ,$$

$$(i = 1,2,\ldots,I_m;\ m = 1,2,\ldots,M).$$

§7.4 Role of Spot Sensitometry.

Spot sensitometry is sometimes used in the more intractable case of photography. Portions of the field are exposed to sources of light "S" of:

(7.4.1) $$m = 1,2,\ldots,M,$$

different brightnesses. To forestall reciprocity failure, the duration of the sensitometric exposures must equal the integration time T; and to avoid contamination, the calibration spots must be placed on a shielded portion of the field.

In the case of the UKST (United Kingdom Schmidt Telescope; Tritton 1983), the illumination is automatically switched on and off as the telescope shutter opens and closes; thus calibration spots are inserted under environmental conditions identical to those for the main field. Illumination is provided both (a) by projectors powered by tungsten lamps that provide seven steps arranged sequentially on two edges of the field, and (b) by a projector of the Kitt Peak design powered by a quartz-halogen lamp with a color correction filter that provides sixteen steps arranged in a square. The intensity of illumination may be varied to suit the exposure at hand.

Following §6.3, let the energy deposited in the m^{th} exposure be the difference between the energy recorded and that contributed by the detector, viz.:

(7.4.2) $$Q_m(S_m) = Q_m(S_m+d) - Q_m(d) \ .$$

The notation of equation (7.4.2) is simplified by omission of the bandpass argument, the solid angle of the exposure (inasmuch as averages over large numbers of pixels $j = 1,2,\ldots,J$ can be made), and the primes on j (since detector contributions can only be assessed from pixels suitably near the spots). In the case of photography, energies on the r.h.s. of equation (7.4.2)

may be rewritten with the help of equation (7.1.2); i.e.:

$$(7.4.3) \qquad Q_m(S_m) = \sum_{n=1}^{N} C_n^{(o)} \left[P_{nm}\{D(S_m+d;p)\} - P_{nm}\{D(d;p)\} \right] ,$$

where the extra polynomial subscript m is inserted without confusion to signify the spot under consideration (i.e. P_{nm} still signifies P_n, but for spot m).

Equation (7.4.3) can be put to a variety of uses. Energies Q_m may be known (a) absolutely, or (b) relatively; and in either case, that information may or may not be used in conjunction with calibration from standard stars. The more common (indeed perhaps the only) real case is that of relative calibration, but the analysis proceeds naturally from the former.

(a) Absolute Calibration.

If Q_m is known absolutely, then equation comprises M equations in N unknown coefficients, which by equation (7.1.6) are:

$$(7.4.4) \qquad C_n^{(o)} = C_n \, A_e T \, 10^{0.4m^{(o)}} .$$

Substitution into equation (7.4.3) reveals the connection between the absolute energy of calibration and the magnitude zero-point [e.g. equation (6.3.9)]; thus it is reduced to dimensionless form:

$$(7.4.5) \qquad Q_m(S_m) \, 10^{-0.4m^{(o)}} (1/A_e T) = \sum_{n=1}^{N} C_n \left[P_{nm}\{D(Sm+d;p)\} - P_{nm}\{D(d;p)\} \right] .$$

If Q_m is known, then equation (7.4.5) provides M equations in N unknowns C_n. Since N might be perhaps 3 or 4 at most, the linear system would be overdetermined for the 7 to 16 spots available on UKST plates.

(b) Relative Calibration.

More reliable information is available from the ratios of supplied energies. Take ratios conveniently (with respect to Q_M, say) and let:

$$(7.4.6) \qquad R_{mM}(S_m,S_M) = Q_m(S_m)/Q_M(S_M) .$$

Then:

$$(7.4.7a) \qquad R_{mM}(S_m,S_M) = \frac{\sum_{n=1}^{N} C_n \left[P_{nm}\{D(S_m+d;p)\} - P_{nm}\{D(d;p)\}\right]}{\sum_{n=1}^{N} C_n \left[P_{nM}\{D(S_M+d;p)\} - P_{nM}\{D(d;p)\}\right]} \text{ , } (m=1,2,\ldots,M-1)$$

or on rearranging terms (and suppressing argument D for simplicity):

$$(7.4.7b) \qquad \sum_{n=1}^{N} C_n \left[R_{mM}\{P_{nM}(S_M+d)-P_{nM}(d)\} - \{P_{nm}(S_m+d)-P_{nm}(d)\}\right] = 0 \text{ .}$$

Since relative calibration is sought, only ratios of coefficients need to be found. Let:

$$(7.4.8) \qquad K_{nN} = C_n/C_N = C_n^{(o)}/C_N^{(o)} \text{ , } (n=1,2,\ldots,N-1) \text{ .}$$

Equations (7.4.7a,b) are then:

$$\sum_{n=1}^{N-1} K_{nN} \left[R_{mM}\{P_{nM}(S_M+d)-P_{nM}(d)\} - \{P_{nm}(S_m+d)-P_{nm}(d)\}\right]$$

$$(7.4.9) \qquad = \{P_{Nm}(S_m+d)-P_{Nm}(d)\} - R_{mM}\{P_{NM}(S_M+d)-P_{NM}(d)\} \text{ ,}$$

$$(m = 1,2,\ldots,M-1).$$

As noted above, relative spot sensitometry may be used in conjunction with calibration from standard stars, or independently. The two cases are represented by equations (7.4.7b) and (7.4.9) respectively.

When both standard stars and spot sensitometry are available, equation (7.4.7b) comprises an additional M-1 equations for simultaneous use with system (7.1.9); or it may be inserted simultaneously into the perturbed system (7.2.6) as part of the iteration procedure. Alternatively, equation (7.4.9) is an overdetermined linear system in (N-1) unknown relative calibration coefficients whose solution gives the shape but not the zero-point of the calibration curve. Relative surface brightnesses may be obtained, but rough absolute brightnesses may be inferred even if there is only one standard star in the field.

§7.5 Calibration from Space.

In the absence of atmospheric emission and extinction, equation (7.1.9) still holds, except that terms must be reinterpreted.

$m_{o,i}(*)$ is the magnitude of source i attenuated only by the interstellar medium; [corrections for interstellar extinction are not considered here.]

M(z) is the relative interplanetary mass at angle z measured toward the ecliptic. Extinction coefficients k_1, k_2, and k_3, pertain now to the interplanetary medium. The integrated source function of equation (6.1.5) manifests itself as contributions "s" to the analog outputs D.

§7.6 Reciprocity Failure

Reciprocity failure (RF) refers to the failure of a detector to maintain a reciprocal relation between illumination I and integration time T in the definition of 'exposure':

$$E = IT \ . \tag{7.6.1}$$

A given exposure obtains as long as I and T are inversely proportional to one another, but the detector might not respond identically in all cases. Photographic emulsions are particularly susceptible.

Wide-angle cameras employ photographic emulsions as the detector of choice in the study of large scale phenomena. In the case of comets with high proper motion, the existence of morphologically interesting structures can best be seen when the camera tracks the comet. Unfortunately, if photometric data are to be extracted as well, standard stars will appear trailed relative to the comet image. In this case, the detector is exposed to various levels of light for different periods of time, so RF may manifest itself in different responses to high I for short T than to reciprocally low I for long T. This section comprises (i) the description of the problem of RF stripped of extraneous complexity, followed by (ii) a scheme to overcome the difficulties.

On suppressing the argument of bandwidth β, equations (6.3.8), (7.1.4) and (7.1.5) give:

$$\begin{aligned} Q_j(\omega_j,z;*) &= A_e T \, 10^{-0.4[m_o(\omega_j;*) - m^{(o)} + k_1 M(z) + k_2 \Gamma_o M(z) + k_3 M^2(z)]} \\ &= \sum_{n=1}^{N} C_n^{(o)} \, [P_{n,j}\{D_j(*+s+d);p\} - P_{n,j'}\{D_{j'}(s+d);p\} \\ &\qquad - P_{n,j}\{D_j(d);p\} + P_{n,j'}\{D_{j'}(d);p\}] \ . \end{aligned} \tag{7.6.2}$$

To reveal the essence of RF, assume no detector noise, no atmospheric extinction or emission, and a single pixel solid angle. Moreover, it suffices that the detector response be represented by a function P[D(*)]. For a star "i", equation (7.6.2) is:

$$(7.6.3) \qquad Q(*_i) = P[D(*_i)] = A_e T \, 10^{-0.4[m(*_i)-m^{(o)}]} .$$

In terms of illumination:

$$(7.6.4) \qquad I(*_i) = Q(*_i)/A_e T = P[D(*_i)]/A_e T = 10^{-0.4[m(*_i)-m^{(o)}]} .$$

In terms of exposure:

$$(7.6.5) \qquad E(*_i) = I(*_i)T = Q(*_i)/A_e = P[D(*_i)]/A_e = T \, 10^{-0.4[m(*_i)-m^{(o)}]} .$$

Perform a thought experiment in which two point sources are detected, one trailed and the other not. Assume that the trailed source results from faithful guiding on the untrailed source, but that it has zero albedo except for a spot that is a specular reflector. The trailed source "t" (a rotating black asteroid with a mirror?) is detected as a series of starlike images, whereas the guided source "g" (a fixed star tracked at the sidereal rate?) is detected as a single image. The exposure time T_t of a single image of the trailed source is therefore shorter than the exposure time T_g of the guided source:

$$(7.6.6) \qquad T_t \ll T_g .$$

Suppose next that sources "t" and "g" have the same exposure E, so that source "t" would have a brighter image if it were not trailed; i.e.:

$$(7.6.7) \qquad m(*_t) < m(*_g).$$

The same energy is detected in the brighter source in the shorter time, as is detected in the fainter source in the longer time. Then if there were perfect reciprocity between I and T:

$$(7.6.8) \qquad \frac{E(*_t)}{E(*_g)} = \frac{I(*_t)T_t}{I(*_g)T_g} = \frac{Q(*_t)}{Q(*_g)} = \frac{T_t \, 10^{-0.4m(*_t)}}{T_g \, 10^{-0.4m(*_g)}} = \frac{P_t[D(*_t)]}{P_g[D(*_g)]} = 1.$$

The first four ratios are all unity by agreement and by definition of physical quantities, but the last ratio is unity only if the subscripts make no difference; i.e. in the absence of RF:

$$P_t[D(*_t)] = P_g[D(*_g)] \tag{7.6.9}$$

In other words, the quantity D for the brighter image "t" detected over a shorter time would equal D for the fainter image "g" detected over a longer time, and the perfect detector would have a common response P(D) under all circumstances.

On the other hand, if RF exists, then:

$$P_t[D(*_t)] \neq P_g[D(*_g)]. \tag{7.6.10}$$

In the experiment at hand, the problem can be handled only if a way is found to relate P_t to P_t. This translates into different polynomial summations for the r.h.s. of equation (7.6.2), except that with atmospheric absorption and emission, the sky brightness and detector noise components are not subject to RF to a first approximation.

The general problem is even more difficult owing to the fact that a trailed star image, blurred by seeing, is subject also to the Fog and Intermittency Effects. In the former effect, the leading parts of the trailed image pre-expose and pre-sensitize the detector, while in the latter effect, parts of the trail are intermittently exposed to equal brightnesses of the trailing image (except in the extreme lateral edges). Couple these and other likely effects, with the fact that RF is itself highly variable, and it is clear that photometric programs on faint structures in high proper motion objects must be designed with paramount emphasis on photometric control.

It is not sufficient merely to apply equal but oppositely directed trailing to both standard stars and comet by tracking at a rate equal to the sidereal rate plus half the proper motion rate. Not only will a great deal of

morphological information be lost or difficult to retrieve; but the photometry of a trailed point source will not be the same as the photometry of a diffuse source, because the point source will trail onto parts of the detector pre-exposed merely to the sky, whereas parts of the diffuse source will trail onto other parts of itself, as well as the sky.

It is equally unsatisfactory to rely solely on sensitometry spots, for while these are certainly helpful in acquiring relative brightnesses of the guided source, they do not necessarily provide the zero-point of the photometry in a reliable way. Moreover, if they are available at all, sensitometry spots are often applied under environmental conditions different than those of the main exposure.

We suggest that there is only one genre of solution to the problem, with two chief variants. The underlying principle is well-known, viz. that the existence of strict controls and the use of standard stars is the only way to do absolute photometry. The variants divide along the following lines, according as sensitometry spots are (a) utilized or (b) unavailable.

(a)

If sensitometry spots are available, then the goal is to use standard stars to calibrate them! Standard stars are therefore the indirect absolute calibrators, and the best ones at that. A series of exposures of standard star fields would be made, and spots inserted, under variable environments but with identical integration times. Ideally, the laboratory conditions must be equal to the outside environment, and spot intensities must be strictly reproducable. All emulsions would be from the same batch, be developed together, and otherwise be subject to egalitarian treatment throughout. Data reduction would follow the lines of §7.4. There would be no RF problem, and indeed no need for standard stars to be in the field of the comet. [If there are standards in the

field, so much the better, for then they can be used to develop a library of RF solutions (7.6.10) as a function of exposure time, incident radiance, and detector type.] Several series through the night will monitor possible changes in extinction and sky brightness. If the opportunity window is limited, then the comet photometry should at least be bracketed by spot calibration. RF can be beaten by use of a detector whose unsusceptibility can be demonstrated via (a) above. Failing this, there is (we suggest) only one recourse.

(b)

If sensitometry spots are unavailable, a scheme must be devised to avoid the trailing of the calibrating stars. Just as sensitometry spots are inserted onto the main exposure in a separate procedure, so standard stars (which now take the place of the spots) must be inserted separately. The basic maneuver is to allocate a potion of the detector for guided standard stars at the same mean zenith distance as the guided comet, which is exposed separately onto the rest of the detector. This can be accomplished by masking the relevant part of the detector during each exposure. Each exposure has identical integration times, and is made as soon as possible one after the other. Any trailed stars in the field of the guided comet are then photometrically irrelevant. The net effect is to have one's cake and eat it, for there will then exist a direct comparison between guided photometric standards and the guided comet. The assumptions are the same as those that obtain conventionally: that (i) the detector is uniform, and (ii) sky brightness and environmental conditions do not change from one part of the procedure to the next. Concerning (i), a lack of detector uniformity manifests itself as random and systematic error. In the conventional technique, random error appears as noise in the calibration, and systematic error can be ascertained from subsets of standards across the detector. In the new technique, the role of random and systematic errors is the same for the stand-

ard star exposure, but a systematic error across exposures can only be inferred by extrapolation and inference. Again, the need for controls is apparent, and is here accomplished by reversing the sequences of exposures, with rigid adherence to the maxim 'ceteris paribus'. As to environmental conditions (ii), their equality in the new technique is easier to accomplish and to monitor, since calibration is actually accomplished at the telescope rather than in the laboratory.

Clearly, these options require a well-designed and executed observing program, but this is expected.

VIII. POLYNOMIAL PROPERTIES

§8.1 BAKER-SAMPSON POLYNOMIALS

The standard rectification function of Baker (1926) and Sampson (1926) has the form $(10^D-1)^p$, where D is the specular photographic density and p is positive. The generalized polynomial expansion is:

$$P = \sum_{n=1}^{N} C_n(10^D-1)^{pn} \quad . \tag{8.1.1}$$

At least one coefficient C_n must be positive in order that P be positive in any specified domain of interest of (D,logP). Any component $P \sim (10^D-1)^{pn}$ tends to zero as D^{pn}. It is the low numbered terms in the expansion that govern the low D asymptote and thus emulate the low density part of the H&D curve. Evidently, the lowest numbered coefficient must be positive for real exposures.

At large D, the n^{th} term increases as:

$$P \sim 10^{Dpn} \quad , \tag{8.1.2}$$

so that:

$$dD/d\log P = 1/pn \quad . \tag{8.1.3}$$

This is the slope of the high D asymptote, which is less for greater p and n. Thus for a given p in equation (8.1.1), the last term in the expansion:

$$C_N(10^D-1)^{pN}$$

governs the final slope of the polynomial expansion, regardless of the size of C_N. In fact, if C_N is negative, P may eventually turn negative, and its logarithm is then imaginary. This is the opposite of what is required to model saturation and the approach to solarization.

The condition for a maximum in logP vs. D may be derived by considering the competition between only two terms, viz. the last one of the expansion and any antecedent term, since it is the last term which will ultimately cause the modelled H&D curve to 'turn over' while the antecedent term attempts to model

the low density asymptote correctly. Let the terms have expansion numbers m and n (m < n). Physical meaning obtains only when P > 0 and D > 0; i.e.:

$$P = C_m(10^D-1)^{pm} + C_n(10^D-1)^{pn} > 0, \quad (D > 0). \tag{8.1.4}$$

A maximum will exist in logP when dlogP/dD = 0; but since P is itself never zero or infinite in the domain of interest, the condition is dP/dD = 0. Thus:

$$mC_m(10^D-1)^{pm} + nC_n(10^D-1)^{pn} = 0 \ . \tag{8.1.5}$$

Dividing equation (8.1.5) by m and subtracting from equation (8.1.4) gives:

$$(1 - \tfrac{n}{m})\ C_n\ (10^D-1)^{pn} > 0 \ . \tag{8.1.6}$$

Thus $C_n < 0$ since $n > m$, and the condition for a real maximum in logP is:

$$p > 0,\ n > m,\ D > 0,\ P > 0;\ C_m > 0,\ C_n < 0 \ . \tag{8.1.7}$$

Condition (8.1.7) alone is insufficient to guarantee a respectable range of D for which logP is real; normally one expects to model a range of densities up to, say, 3 or 4. This imposes a further restriction on the magnitude of the coefficients. The value D_{max} at which a maximum in logP will occur is governed by equation (8.1.5), which can be rewritten as:

$$10^{D_{max}} = 1 + (-mC_m/nC_n)^{1/p(n-m)} \ . \tag{8.1.8}$$

But any respectable value of D_{max} must be such that 1 makes a negligible contribution to the r.h.s. There is therefore a practical constraint on the ratio of coefficients given by:

$$p(n-m)D_{max} \sim \log(-nC_n/mC_m), \quad (D_{max} >> 1,\ C_n < 0,\ n > m). \tag{8.1.9}$$

For example, if m=1, n=2, p=0.25, $D_{max} = 4$, equation (8.1.9) requires that:

$$|C_2| \sim C_1/20.$$

In general, in the event that the last coefficient of the expansion is negative, and in order for a substantial area of the (D>0,logP) plane to be occupied by real solutions:

$$|C_n| << C_m, \quad (n > m,\ C_n < 0). \tag{8.1.10}$$

§8.2 SATURATION AND INFLECTION

When all coefficients in equation (8.1.1) are positive, then the entire (D>0,logP) plane is occupied by real solutions. The resulting curve is wobbly, but the simplest wobble is an inflection that results from the competition between two terms of the series, say m and n<m. Results of the previous section show that the lower order term governs the low D solution, and the higher order term governs the high D solution; the low order coefficient C_m must always be positive, and when the higher order coefficient C_n is negative it produces a maximum in logP. But when the higher order coefficient C_n is positive, it produces a slope of 1/pn which is less than the slope 1/pm. Consequently, inflection will always occur as a flattening with increasing D, and this is now ultimately the correct form by which to account for saturation.

The condition for inflection is $d^2\log P/dD^2 = 0$. For two terms, P is given by equation (8.1.4), viz.:

$$P = C_m(10^D-1)^{pm} + C_n(10^D-1)^{pn} \quad . \tag{8.2.1}$$

Thus points of inflection occur whenever D satisfies:

$$[m + nC(10^D-1)^{p(n-m)}][1 + C(10^D-1)^{p(n-m)}] = pC\,(n-m)^2\,10^D\,(10^D-1)^{p(n-m)}, \tag{8.2.2}$$

where:

$$C = C_n/C_m \quad . \tag{8.2.3}$$

Condition (8.2.2) is better written as a quadratic in C:

$$m + C[m+n-p(n-m)^2 10^D](10^D-1)^{p(n-m)} + C^2 n(10^D-1)^{2p(n-m)} = 0. \tag{8.2.4}$$

It suffices merely to consider the case m=1, n=2. Then equation (8.2.4) is:

$$1 + C[(3-p10^D)(10^D-1)^p] + C^2[2(10^D-1)^{2p}] = 0, \tag{8.2.5}$$

which has roots:

$$C = [p10^D-3\pm\sqrt{1-6p10^D+p^2 10^{2D}}]/4(10^D-1)^p \quad . \tag{8.2.6}$$

These roots are real whenever:

(8.2.7) $$p^2 10^{2D} - 6p10^D + 1 \geq 0 \ .$$

Let Y be $p10^D$. Then:

(8.2.8) $$[Y-(3+2\sqrt{2})][Y-(3-2\sqrt{2})] \geq 0 \ .$$

For the inequality to hold, each factor must have the same sign; either:

$$Y-(3+2\sqrt{2}) \geq 0 \quad \text{and} \quad Y-(3-2\sqrt{2}) \geq 0,$$

or:

$$Y-(3+2\sqrt{2}) \leq 0 \quad \text{and} \quad Y-(3-2\sqrt{2}) \leq 0.$$

In other words:

(8.2.9) $$3-2\sqrt{2} \geq Y \geq 3+2\sqrt{2} \ .$$

Consider each limit in turn.

For the upper limit $Y \leq 3-2\sqrt{2}$ of equation (8.2.9), it is easy to show that C is always negative regardless of the sign of the square root in equation (8.2.6). Thus:

(8.2.10) $$p10^D \leq 3-2\sqrt{2} \ ,$$

corresponds always to negative C. From the previous section, these are pathological H&D curves that first show inflection, before ultimately reaching a maximum in logP and reversing course.

For the lower limit $Y \geq 3+2\sqrt{2}$ of equation (8.2.9), regardless of sign in equation (8.2.6), C is always positive. Thus:

(8.2.11) $$p10^D \geq 3+2\sqrt{2} \ ,$$

is the more desirable case, since inflection bends the solution in direction of increasing logP. Two roots for C are ensured by the two signs in equation (8.2.6), except when the equality holds, in which case:

(8.2.12) $$C = (p10^D-3)/4(10^D-1)^P \ .$$

The array of permissible values of C, and the densities at which they occur, are displayed in Table 8-1 for positive C, and in Table 8-2 for negative C.

Table 8-1.

Values of log C ($C = C_n/C_m > 0$, n=m+1=2) for which inflection occurs in a curve modelled by the Baker-Sampson polynomial expansion: $C_m(10^D-1)^{pm} + C_n(10^D-1)^{pn}$.

D	p = 0.1		p = 0.2		p = 0.4	
5	3.1988	-4.4500	2.9999	-5.3009	2.3010	-6.6020
4	2.2977	-3.3987	2.1994	-4.1004	1.7007	-5.2017
3	1.3857	-2.2866	1.3935	-2.8944	1.0979	-3.7986
2	0.3259	-1.0257	0.5273	-1.6265	0.4683	-2.3658
1.7656	-0.3263		0.2727	-1.2770	0.3015	-2.0090
1.5	-		-0.1941	-0.7031	0.0794	-1.5693
1.4645	-		-0.4404		0.0445	-1.5050
1.25	-		-		-0.2408	-1.0401
1.1635	-		-		-0.6036	
1	-		-		-	
0	-		-		-	

Table 8-2.

Values of C ($C = C_n/C_m < 0$, $n = m+1 = 2$) for which inflection occurs in a curve modelled by the Baker-Sampson polynomial expansion: $C_m(10^D-1)^{pm} + C_n(10^D-1)^{pn}$.

D	p = 0.1		p = 0.15		p = 0.17	
0.3	-		-		-	
0.2344	-0.7312		-		-	
0.2	-0.6777	-0.8214	-		-	
0.1	-0.6764	-0.9685	-		-	
0.05836	-0.7023	-1.0493	-0.9458		-	
0.05	-0.7112	-1.0707	-0.9239	-1.0172	-	
0.01	-0.8258	-1.2843	-1.1100	-1.3915	-	
0.00400	-0.9036	-1.4116	-1.2667	-1.6084	-1.5676	
0.001	-1.0372	-1.6239	-1.5556	-1.9872	-1.9287	-2.0435
0.0001	-1.3055	-2.0452	-2.1958	-2.8100	-2.8419	-3.0353

IX. NUMERICAL TESTS.

§9.1 Input Data

Verification of the theory of Zou, Chen, Peterson (1981) has been accomplished by these authors themselves, and by Klinglesmith and Rupp (1984), and Speck et al. (1987), using M31. These works were concerned solely with derivation of the polynomial coefficients, and did not address the problem of the derivation of the extinction coefficients and sky brightness. Walterbos and Kennicut (1987) also studied M31, but relied solely on laboratory calibration. Warnock and Klinglesmith (1984) have worked on the problem of trailed standards.

As a first step in the development of a data reduction algorithm for the general theory of standard star calibrators, it is necessary to formulate a problem that will serve to test it and to reveal its numerical properties. We seek to answer the general questions: (i) does the theory work in principle, and in particular, can the primary extinction coefficient be derived? and (ii) are the numerical techniques satisfactory, and what are their properties?

In order to accomplish this first step, it is necessary to input densities that are reasonable facsimiles of data to be expected in real cases. Since the data available for M31 had standard stars grouped over a very narrow range of zenith distance (cf. Speck 1987), and were moreover secured at small zenith distance, they were unsuited to a test for a complete solution. With the help of sensitometric densities taken from UK Schmidt plates, and from our prior analysis of M31, a canonical data-set was established comprising 9 stars divided into 2 groups; stars #1 - #4 were located at zenith distance $z = 60°$, and stars #5 - #9 were located at $z = 66°$. The input data are summarized in Table 9-1. The division into two groups is necessitated by the fact that the primary extinction coefficient cannot be determined unless there is a sufficiently large range of z (§6.4). The chosen range of 6° is large enough

to eliminate any numerical effects owing to ill-determined matrices, yet small enough to correspond to any reasonable range of z accessible to wide-field cameras. The background sky + fog contribution was established for each group of stars, and the background fog contribution, assumed uniform over the field, was similarly fixed.

Each standard star, sky, and fog frame was comprised of 10 x 10 pixels. The number of square arc seconds subtended by a pixel is given by:

$$a = (0.001\ l\ s)^2$$

where l is the pixel length in microns, and s is the plate scale in "/mm. For values of l = 20 microns/pixel and s = 100 "/mm, a is 4 sq. arc seconds/pixel. Star image sizes were determined from the formula of Liller and Liller (1975) pertinent to Palomar 1.2m Schmidt plates. In all cases, air masses were simply equated to sec z. All input data are therefore well within range of normal expectation.

§9.2. Tests of the Algorithm.

Since the primary extinction coefficient is far and away the most important one, the primary goal is to see whether there is a reasonable expectation of its derivation. We describe here the results of tests which are the simplest conceivable, yet which are still definitive; viz. tests of the case where (i) the tertiary extinction coefficient is ignored, (ii) the secondary color coefficient is assumed known, and (iii) only the primary coefficient and one or two Baker-Sampson polynomial coefficients are regarded as unknowns. Thus the inclusion of the secondary color coefficient and stellar color indices (CI) in Tables 9-2 and 9-3 are for present purposes to be regarded as non-participatory factors insofar as the present tests are concerned, even though their values were used to evaluate participatory coefficients [e.g. the l.h.s. of equation (7.2.2)].

When there is only one polynomial coefficient C, the problem (7.2.2) becomes inherently linear in log C and the extinction coefficients, and is thus more amenable to direct analytic treatment (§9.4). For the sake of simplicity, we describe the parallel numerical implementation of Newton's method as if this were the case.

A program in GWBASIC was written to implement the theory of §7.2. Equations (7.2.3a,b) and (7.2.5) were programmed to evaluate the 2 x 9 matrix A of equation (7.2.6), whose 2 columns are necessitated by the 2 unknown corrections to k_1 and the polynomial coefficient C in matrix X, and whose 9 rows correspond to the 9 standard stars. Similarly, the 9 rows of matrix Y of equation (7.2.6) are evaluated at each iteration for each of the 9 standards. Evaluation of the matrix $(A^TA)^{-1}A^T$ proceeds by the usual means (e.g. Natrella 1963; but note that matrix elements there are opposite to the conventional RC - or Row/Column - notation!); this matrix will be merely 2 x 2 if there are

only 2 unknown coefficient corrections X. In double-precision, the solution of equation (7.2.6) can be found by implementing Cramer's Rule without fear of ill-conditioning; our results show that Cramer's Rule works for 2 or 3 unknowns. In the case of more unknowns, more sophisticated methods are necessary (e.g. Branham 1988).

To demonstrate the numerical accuracy and correctness of the program, we have evaluated the magnitudes m_i appearing in the terms of matrix Y [i.e. the r.h.s. of equation (7.2.5), $i = 1,2,\ldots,9$] such that each term is zero. This ensures that the the optimization parameter p, and the coefficients k_1 and C, used in the calculation, should be the ones that obtain after implementation of the iteration algorithm. Double precision is used throughout, with results given in Table 9-2. When the iteration algorithm is then run to convergence, the results shown in Figures 9-1 and 9-2, and in Table 9-3, are found; the input data are recovered, so the program works correctly and with sufficient accuracy (at least 5 significant figures). Moreover, the test shows that the range in z is sufficient to ensure that the determinant A is well-conditioned.

For the test data used here, and for p in the range of about ±0.05 about the correct value, improvement in the coefficients is found at a rate of an order of magnitude or more per iteration. Farther from the correct value of p, convergence is slower as expected, and is marked by two requirements: (i) the guessed value must be closer to the correct one for convergence to occur, and (ii) it is necessary to settle for fewer significant figures before divergence sets in. Ultimately, the requirement (i) above becomes absurdly stringent, and for all practical purposes the trial solutions diverge. This quantifiable behaviour is canonical, and is programmable in the general case.

Owing to the linear properties of the perturbed system, k_1 converges

at a rate that keeps pace with the polynomial coefficient C, and this means that it must be derived formally to an accuracy unwarrented by the observations if C is to be accurate to, say, 4 significant figures. It is to be expected that a similar condition obtains in the general case, and in fact it might be quite satisfactory simply to regard k_2 (and perhaps k_3) as given. This should substantially improve the convergence properties of the algorithm in the general case by allowing every bit of information from the standards to contribute where their need is greatest, viz. in the determination of k_1 and the polynomial coefficients.

§9.3. Magnitude Errors

Standard star magnitudes will cutomarily be in error, and these may be systematic or random. The effects of random error in a given number of standards will be to reduce the ability of the algorithm to converge; this can be surmised by carrying the argument to the extreme, when input magnitudes in equation (7.2.5) are so poor that the polynomial differences there are incapable of reproducing them. Random error is meliorated by increasing the number of standards, but the errors must continue to be randomly distributed in zenith distance as well if k_1 is to be accurately determined.

Table 9-3 contains solutions for two worst cases in the case of 9 standard stars: viz., when the same absolute error of 0.03 mag is systematically distributed in z, such that (i) all m_i are too large (i.e. too faint) at the smaller z, and too small (i.e. too bright) at the larger z; and (ii) vice versa. In the test case here (Tables 9-1, 9-2) the set at smaller z contains 4 stars, and the set at larger z has 5 stars, so that the median of the random errors is as close to zero as needed for this illustration.

The convergence properties in these two cases are shown in Figure 9-2. The upper and lower curves are the envelopes which contain all other solutions resulting from any other z-distribution of error (provided the absolute error is still 0.03 mag and the choices of z are as stated). In other test cases not reported here, convergence is slowed by larger magnitude errors, as expected, until finally for large enough errors there is a failure to converge. The numerical results confirm that the algorithm is able to handle situations where, owing to observational error or differences in system response, the standard star magnitudes and the observed densities are not always precisely compatible.

The results of Table 9-3 show that when magnitude errors are always positive at the lower z and negative at the higher z, the derived extinction

coefficient is greater than it would be if there were no errors (and vice versa). This may be difficult to see at first glance, but a convincing argument proceeds as follows. If magnitudes at the lower z are perceived as preferentially too faint, i.e. the magnitude errors are positive, then the extinction coefficient would have to be greater to compensate for this. On the other hand, the negative magnitude errors which cause the perceived magnitudes at the higher z to be too bright, do not require a lower extinction coefficient as might be expected, because the air mass is larger there, sufficiently large in fact that the negative magnitude error is accounted for (and vice versa). This result is seen also with the help of an analytic treatment.

§9.4 Analytic Solutions

Reduce the system (7.2.2) to its essentials for two unknowns, k and C:

(9.4.1) $$m_i + kM_i + 2.5 \log C = R_i, \quad (i = 1,2,\ldots,I)$$

where R_i $(i = 1,2,\ldots,I)$ is an abbreviated notation for the polynomial differences in equation (7.2.2), and are assumed known. M = sec z is the air mass. Suppose that equation (9.1.1) is exactly satisfied for all i, i.e. that magnitudes exist in theory which precisely satisfy the system. These "true" magnitudes will presumably differ slightly from the standard star input magnitudes. Suppose that these small differences are the same in absolute value for all i, but are systematically incurred such that:

(9.4.2a) $$m_i(\text{new}) = m_i + dm, \quad (i = 1,2,\ldots,I_1, \; M = M_1)$$

and

(9.4.2b) $$m_i(\text{new}) = m_i - dm, \quad (i = I_1+1, I_1+2, \ldots, I, \; M = M_2).$$

The errors will engender small departures from the "true" coefficients k and C, such that:

(9.4.3) $$k(\text{new}) = k + dk,$$

and:

(9.4.4) $$\log C(\text{new}) = \log C + d\log C,$$

will be the new solution. The r.h.s. of equation (9.4.1) will not change of course. Equations (9.4.1) to (9.4.4) give:

(9.4.5a) $$m_i + dm + M_1(k+dk) + 2.5(\log C + d\log C) = R_i, \quad (i = 1,2,\ldots,I_1),$$

and:

(9.4.5b) $$m_i - dm + M_2(k+dk) + 2.5(\log C + d\log C) = R_i, \quad (i = I_1+1,\ldots,I).$$

When there are no magnitude errors, equation (9.4.1) holds, so that:

(9.4.6a) $$dm + M_1 dk + 2.5\, d\log C = 0, \quad (i = 1,2,\ldots,I_1),$$

and:

(9.4.6b) $$-dm + M_2 dk + 2.5\, d\log C = 0, \quad (i = I_1+1,\ldots,I).$$

Since each system of equations is now independent of i, any one equation from each set suffices to determine dk and dlogC. Thus:

(9.4.7) $$dk = + 2dm/(M_2-M_1),$$

and:

(9.4.8) $$2.5\ dlogC = - dm(M_2+M_1)/(M_2-M_1).$$

It is easily shown that these expressions account precisely for the results in Table 9-3 that have been obtained by numerical implementation of Newton's method.

Equations (9.4.6a,b) reveal another interesting fact that might not be readily apparent. If the signs preceding dm in each equation were to be the same, then dk = 0, but dlogC = ±0.4dm. In other words, if there is a truly systematic error between the standards and the measured responses, regardless of placement in z, then k should still be correctly determined, because k is determined differentially. The systematic error is faithfully transmitted to the photometric expansion coefficient instead. In practice errors will always exist, but if these are normally distributed in z, accurate values for extinction should be derivable to first order, provided that there are enough standards distributed over a sufficient range of z, and provided that the detector is well-behaved for trailed standards. A synopsis of these results has been presented elsewhere (Usher 1989).

Table 9-1

Summary of Input Densities

Zenith Distance	Object	Min.Pix. Density	Max.Pix. Density	Mean Pix. Density	r.m.s. dev.
60°	sky	0.4	0.7	0.550	0.070
	star #1	0.4	1.0	0.574	0.111
	star #2	0.4	2.0	0.651	0.282
	star #3	0.4	2.8	0.763	0.471
60°	star #4	0.4	1.5	0.606	0.171
66°	sky	0.5	0.8	0.650	0.070
	star #5	0.5	2.3	0.749	0.294
	star #6	0.5	3.2	0.905	0.578
	star #7	0.5	1.3	0.668	0.108
	star #8	0.5	1.8	0.697	0.169
66°	star #9	0.5	2.7	0.812	0.375
-	fog	0.2	0.3	0.240	0.049

Table 9-2

Exact Solution Parameters

$p = \frac{1}{4}$; $k_1 = 3/10$; $(k_2 = 0.03)$; $C = 2 \times 10^{-8}$

Star #	mag	CI	z
1	17.63254..	0.5	60°
2	15.93716..	1.0	60°
3	15.01066..	0.9	60°
4	16.67302..	0.7	60°
5	15.71947..	1.3	66°
6	14.59827..	-0.2	66°
7	17.81131..	-0.1	66°
8	16.64795..	1.0	66°
9	15.19134..	0.8	66°

Table 9-3

Summary of Converged Solutions ($k_2 = 0.03$, $k_3 = 0$)

magnitude errors	p	k_1	$Cx10^8$	$m_{sky}(60°)$	$m_{sky}(66°)$	m_{fog}
+/-0.03 (z=60°;66°)	0.25	0.4308	1.5288	22.22	21.93	21.13
0 (exact)	¼	3/10	2	21.93	21.64	20.84
-/+0.03 (z=60°;66°)	0.25	0.1692	2.6164	21.64	21.35	20.55

X. STANDARD STARS FOR THE P/HALLEY APPARITION

§10.1 The Search Area.

The Large-Scale Phenomena Network (LSPN) of the International Halley-Watch has provided large numbers of wide-angle images of P/Halley taken with a variety of cameras located at sites across the world. For the most part, these photographs were taken with instruments that were not equipped with tube spots or calibration wedges, so that calibration must be effected through the use of field stars of known magnitudes and colors. A list of stars of known identification, position, magnitude, and color, has been compiled for this purpose; the entries comprise the Special Halley-watch Identification and Photometric Star Catalog (hereafter, the SHIPSCat) and have been given in a separate report to the LSPN (Dorband and Usher 1985; hereafter, Report II).

In selecting the boundaries of the search area, it was necessary to account for four mutually dependent effects: (i), the angular extent and orientation of the tail; (ii), the sizes of the fields of the network telescopes; (iii), the incidence of calibration standards of the requisite accuracy; and (iv), the centers and orientations of the fields of view of the telescopes along the projected path of the comet. Details of these calculations are given in a separate report to the LSPN (Dorband et al. 1985; hereafter, Report I). Since it was necessary to compile Report I before the event, it was necessary to predict the behaviour of the comet in order to map the availability of standard stars along its path. The geometrical aspect and temporal evolution of the plasma tail was predicted semi-empirically by Niedner (1984) with the help of data from the 1910 apparition. Data on participating telescopes enabled the concept of "average telescope" to be quantified, by which it was surmised that an average field-of-view (FOV) might be comfortably taken to be 50-100 square degrees. As a result, criteria were established with due

consideration for items (i)-(iv) above in order to define the search area. These are discussed in Report I. The final search area is shown in Figure 10-1 and given in greater detail in Report I.

§10.2 Properties of the SHIPSCat.

The question arises as to the incidence of photometric standards that are needed to calibrate a plate to the required accuracy. There is a clear choice: stars with known photographic magnitudes, or stars with known photo-photoelectric magnitudes. The number of photographic standards available per unit surface area of the sky can be estimated from the SAO Star Catalog. Photographic magnitudes are listed for 131,080 stars. These magnitudes lie mainly between 7 and 12. [More than twice as many - almost the full SAO catalog - have visual magnitudes.] The average surface density of photo-photographic magnitudes is thus just over 3 per square degree, providing 300 standards over the 10 degree square FOV of the optimal telescope. The accuracy of these potential standards is unlikely to be better than 0.1 magnitudes, and their usefulness in the implementation of the standard star theory may well be problematical.

On the other hand, the Catalogue of Stellar Identifications (CSI; Ochsenbein 1978; Wenger and Ochsenbein 1984) lists about 6300 objects with U, B, or V, magnitudes over the Halley path (13% of the sky), for an average surface density of about 1.2 per sq. deg. Magnitudes in other systems are far fewer; Geneva photometry amounts to 10% of this value, and is statistically insignificant in the quest for calibration. Stromgren narrow-band magnitudes are the nearest competitor, but the (b-y), m1, c1, and H-beta indices are still only 30% of the broadband magnitudes. Inasmuch as the photographic emulsions likely to be used to record the wide-field phenomena are more similar to the broadband Johnson filters, we confined the search to U,B, and V.

The number of B standards available on a 10 degree square plate is thus about 100, mainly between magnitudes 5 and 13. Considerable numbers of these

may be lost to saturation without hindering a photometric history of P/Halley.

Difficulties in calibration might be encountered only for FsOV of small solid angle, but these are likely to be of less interest to the LSPN. Special cases (such as imagery at high z) may require that the number of standards be supplemented. This can be accomplished either by generating them ab initio, or by generating secondary standards from primary ones. In the first case, high photometric accuracy may be achieved relatively quickly on telescopes of modest aperture with CCD photometry. In the second case, secondary standards with an accuracy of 0.05 mag or better can be generated by the methods outlined.

A minimum of 10 accurate calibrators in an average FOV are necessary to achieve the necessary photometric solution for the large-scale phenomena of interest. Barring setbacks unforeseen by the research effort reported here, the prospects seem excellent for a quantified photometric and morphological history of the latest apparition of P/Halley.

ACKNOWLEDGEMENTS

I thank J.C. Brandt for suggesting this problem. I have benefited from the stimulating discussions that have marked all meetings of the Large-Scale Phenomena Network of the International Halley-Watch. In particular I thank J.C. Brandt, D. Klingelsmith III, W. Liller, M.B. Niedner, and A. Warnock III for their many contributions. This work was supported by NASA Grant NAG 5-361.

BIBLIOGRAPHY

Agnelli, G., Nanni, D., Pitella, G., Travese, D., & Vignato, A., (1979), Ast. Ap. 77, 45.

Baker, E.A., (1925), Proc. R. Soc. Edin. 45, Part II, 166.

Bates, D.M., & Watts, D.G., (1988), "Nonlinear Regression Analysis and its Applications" (John Wiley: New York).

Berg, W.F., (1963), in "Photographic Theory" (London: Focal Press), 173.

Bowen, I.S., (1960), in "Stars and Stellar Systems", Vol I, (Chicago: University of Chicago Press), 43.

Boyd, R.W., (1983), "Radiometry and the Detection of Optical Radiation" (New York: John Wiley).

Brandt, J.C., (1985), communication to the Halley-Watch Large Scale Phenomena Network meeting, NASA-GSFC.

Brandt, J.C., Rahe, J., & Niedner, M.B., (1982), IHW Newsletter 1, 13.

_____ (1982), IHW Newsletter 2, 6.

_____ (1983), IHW Newsletter 3, 24.

Branham, R.L., (1988), QJRAS 29, 399.

Brown, E.B., (1974), "Modern Optics" (New York: Krieger).

Buser, R., (1985), Highlights in Astronomy 7 (ed. J.P. Swings) in press.

Cock, J.P., (1986), Bull. Roy. Obs. Edin. 68, 91.

Dorband, J.E., Usher, P.D., Warnock, A., Klinglesmith, D.A., & Niedner, M.B, (1985), Report to the LSPN of the IHW, "The LSPN SHIPSCat: I. Criteria for the Selection of Standards" (Report I).

Dorband, J.E., & Usher, P.D., (1985), Report to the LSPN of the IHW, "The LSPN SHIPSCat: II. U,B,V, Photometric Standards" (Report II).

Feitzinger, J.V., Nicolov, A., Schmidt-Kaler, T., & Tennigkeit, J., (1983), Ast. Ap. 126, 352.

Garstang, R.H., (1988), Observatory 108, 159.

Golay, M., (1974), "Introduction to Astronomical Photometry" (Dordrecht: Reidel).

Hardie, R.H., (1962), in "Stars and Stellar Systems", Vol. II, (Chicago: University of Chicago Press), 178.

Johnson H.L., (1963), in "Stars and Stellar Systems", Vol. III, (Chicago: University of Chicago Press), 204.

_____, (1966), Ann. Rev. Ast. Ap. 4, 193.

Kalinowski, J.K., Roosen, R.G., & Brandt, J.C., (1975), P.A.S.P. 87, 869.

Klinglesmith, D.A., (1983), "Proc. Astronomical Microdensitometry Conference", Goddard Space Flight Center, NASA Conference Publication 2317.

Klinglesmith, D.A., & Rupp, S.W., (1984), in "Astronomy with Schmidt-Type Telescopes", ed. M. Capaccioli (Dordrecht: Reidel), 155.

Kormendy, J., (1973), Ast. J. 78, 255.

Liller, M.H., & Liller, W., (1975), Ap. J. Letters 189, L101.

Liller, W., (1985), communication to the Halley-Watch Large Scale Phenomena Network meeting, NASA-GSFC.

Mees, C.E.K., (1954), "The Theory of the Photographic Process" (New York: Macmillan), 162.

Minkowski, R.L., & Abell, G.O., (1963), in "Stars and Stellar Systems", Vol. III, (Chicago: Univ. of Chicago Press), 481.

Natrella, M.G., (1963), "Experimental Statistics", US Dept. of Commerce, Nat. Bureau of Standards Handbook 91.

Niedner, M.B., (1984), private communication; Publ. Amer. Ast. Soc. (1915) "Report of the Comet Committee 1909 - 1913".

Niedner, M.B., & Brandt, J.C., (1978), Ap.J. 223, 655.

Ochsenbein, F., (1978), "The Catalogue of Stellar Identifications: Main Features", Bull. Inform. CDS No. 15.

Owaki, N. (1986), Observatory 106, 194.

Pence, W.D., & Davoust, E., (1985), Ast. Ap. Suppl. 60, 517.

Sampson, R.A., (1925), MNRAS 85, 212.

Sandage, A., (1972), Ap. J. 173, 485.

Schoenberg, E., (1929), Handbuch d. Ap. 2, 268.

Speck, S., Usher, P.D., Klinglesmith, D., & Niedner, M.B., (1987), BAAS 19, 684.

Stock, J., & Williams, A.D., (1962), in "Stars and Stellar Systems", Vol. II, (Chicago: Univ. of Chicago Press), 374.

Tritton, S., (1983), U.K. Schmidt Telescope Unit Handbook (Edinburgh: Royal Observatory).

Usher, P.D., (1986), Proc. SPIE 702, 387.

_____, (1987), in "Comets to Quasars" (Cambridge: Cambridge Univ. Press), (in press).

_____, (1989), paper contributed to the colloquium "Comets in the post-Halley era", Bamburg, FRG, 24-28 April 1989.

van der Kruit, P.C., & Searle, L., (1981), Ast. Ap. 95, 116.

Walterbos, R.A.M., & Kennicut, R.C., (1987), Ast. Ap. Suppl. 69, 311.

Warnock, A., & Klinglesmith, D.A., (1984), BAAS 16, 904.

Wenger, M., & Ochsenbein, F., (1984), "SIMBAD V3.0: New Version 1984", Bull. Inform. CDS No. 26.

Wolfe, W.L., (1980), Applied Optics and Optical Engineering Vol. VIII, 117.

Young, A.T., (1974), Methods of Experimental Physics Vol. 12, 95.

Zou, Z-L., Chen, J-S., & Peterson, B.A., (1981), Chin. Ast. Ap. 5, 316.

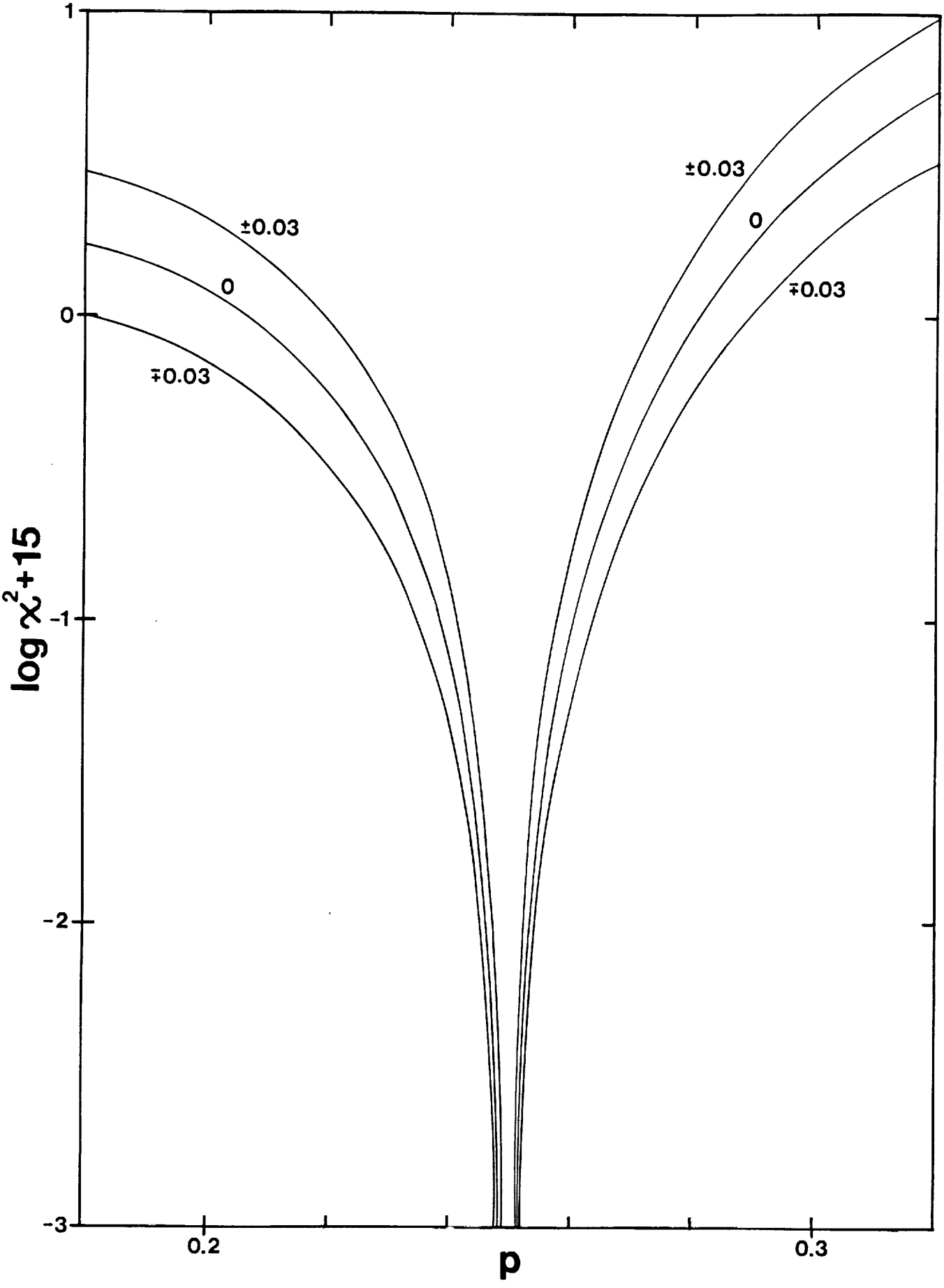

FIG 9-1

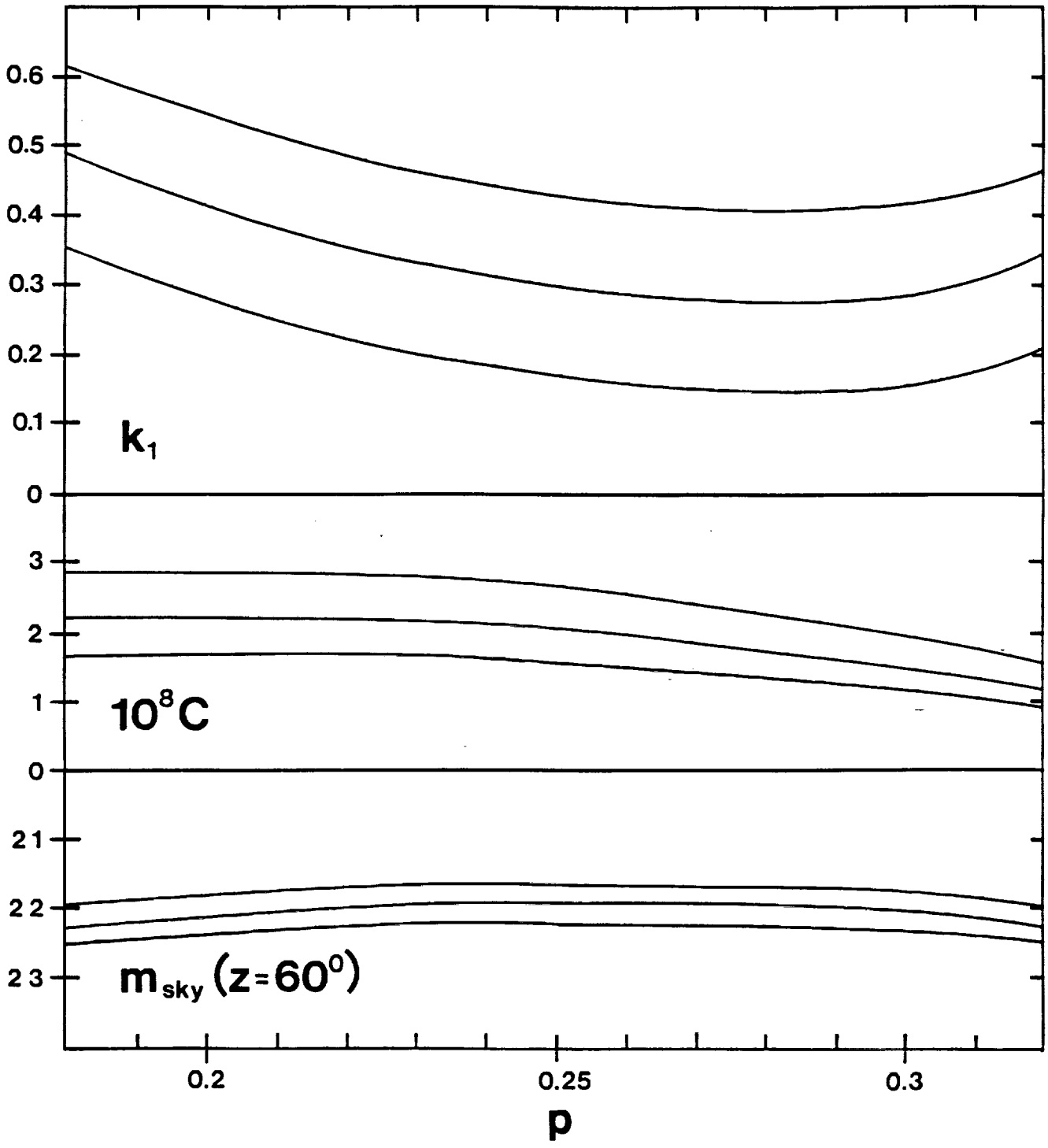

FIG 9-2

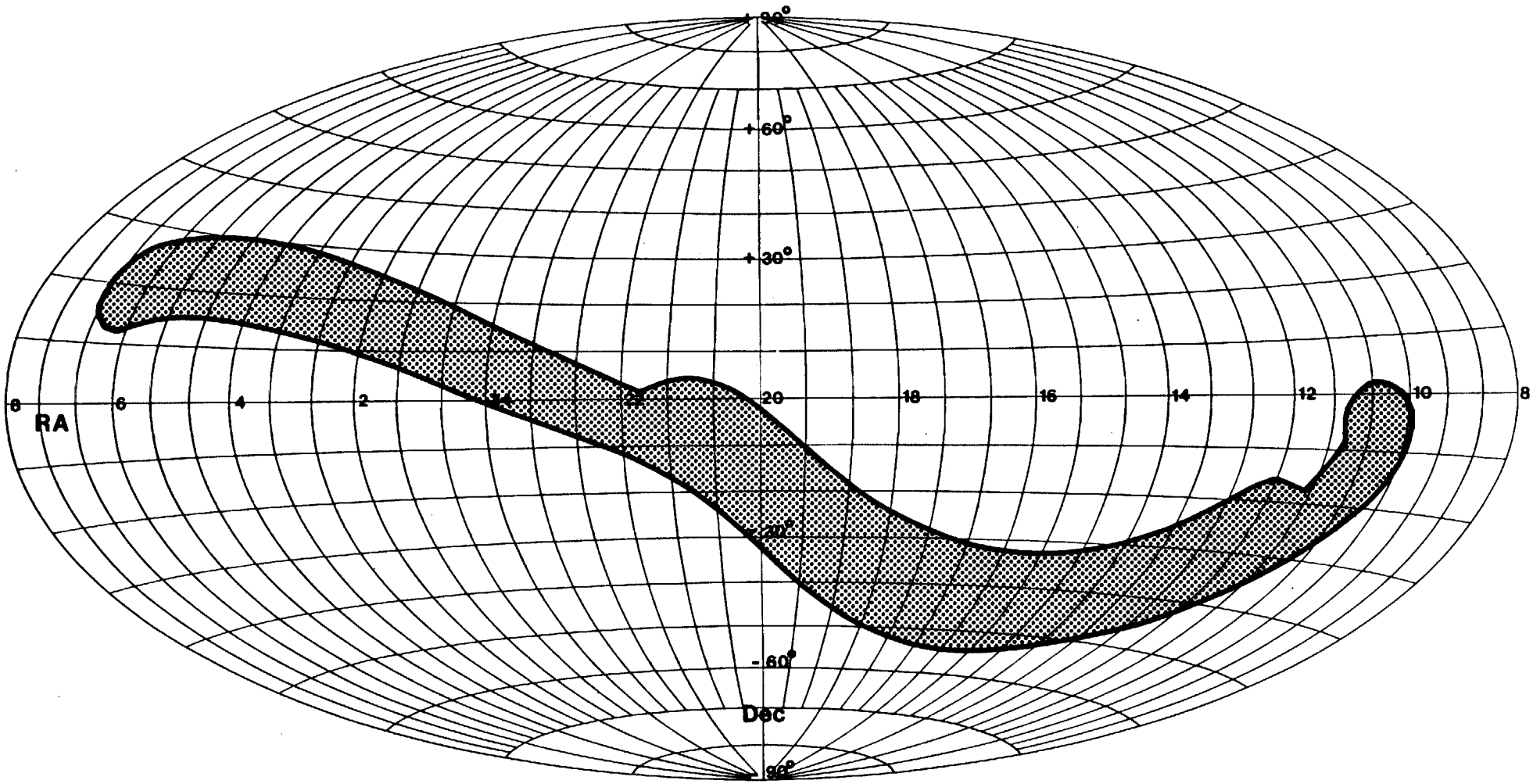

FIG 10-1